

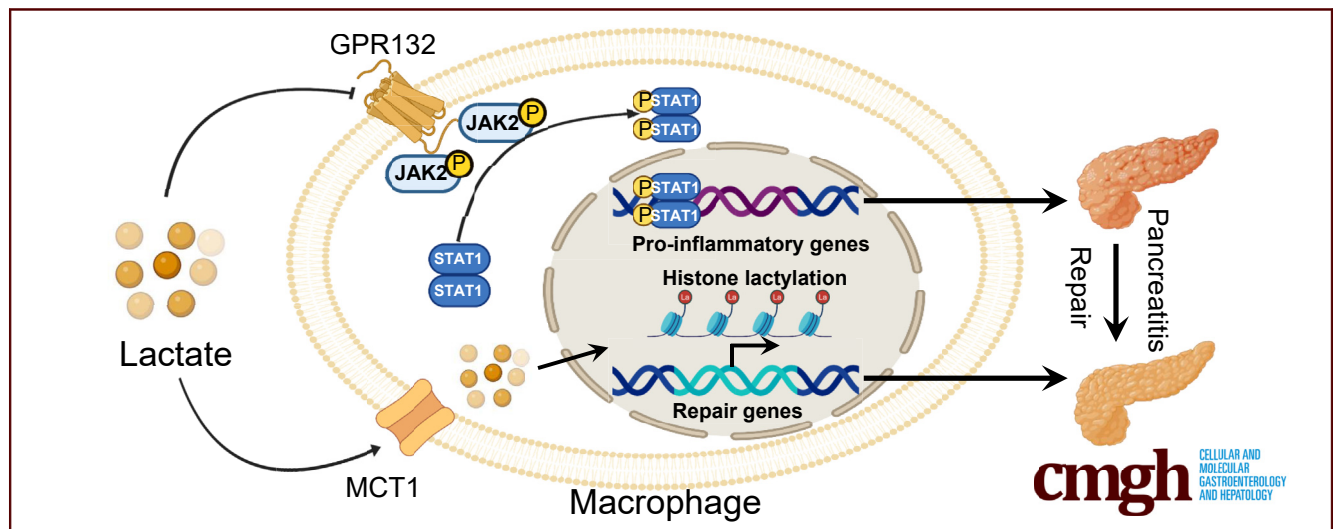
ORIGINAL RESEARCH

Lactate Facilitates Pancreatic Repair Following Acute Pancreatitis by Promoting Reparative Macrophage Polarization



Jing Jiang,^{1,2,*} Ruiyan Wang,^{1,2,*} Pengli Song,^{1,2,*} Qi Peng,^{1,2} Xuerui Jin,^{1,2} Bin Li,^{1,2} Jianbo Ni,^{1,2} Jie Shen,^{1,3} Jingpiao Bao,^{1,2} Zengkai Wu,^{4,5} Xiaolu Ge,² Xingpeng Wang,^{1,2} and Guoyong Hu^{1,2}

¹Department of Gastroenterology, Shanghai General Hospital, Shanghai, China; ²Department of Gastroenterology and Shanghai Key Laboratory of Pancreatic Disease, Shanghai General Hospital, Shanghai Jiao Tong University School of Medicine, Shanghai, China; ³Shanghai General Hospital Jiuquan Hospital, Jiuquan, Gansu, China; ⁴Department of Gastroenterology, Union Hospital, Fujian Medical University, Fuzhou, Fujian, China; and ⁵Fujian Clinical Research Center for Digestive System Tumors and Upper Gastrointestinal Diseases, Fuzhou, Fujian, China



SUMMARY

Lactate promotes reparative macrophage polarization, achieved through promoting lactylation and inhibiting JAK2-STAT1 signaling pathway. The phenotypic change of macrophages alleviates inflammation and improves the inflammatory immune microenvironment, ultimately facilitating pancreatic recovery following acute pancreatitis.

BACKGROUND & AIMS: During acute pancreatitis (AP), glycolysis is enhanced. The upregulation of glycolysis increases the level of metabolite lactate. Lactate has been shown to facilitate tissue repair across various pathologic conditions. However, its role in the recovery following AP remains unclear. This study aims to explore the role of lactate in the regenerative processes following AP and to elucidate its underlying molecular mechanisms.

METHODS: The caerulein-induced recovery AP model was established using wild-type and 6-Phosphofructo-2-Kinase/Fructose-2,6-Biphosphatase 3 (Pfkfb3) heterozygous mice. Pancreatic repair was evaluated histologically, whereas lactate levels and inflammatory markers were measured serologically.

Macrophages were isolated from pancreatic tissue using fluorescence-activated cell sorting for mRNA sequencing to identify phenotypes. In ex vivo, macrophages were indirectly co-cultured with inflammatory acinar, and the effect of lactate on macrophage phenotype were investigated through immunoprecipitation, fluorescence analysis, and Western blotting.

RESULTS: We first found that exogenous lactate administration promoted pancreatic repair, whereas *Pfkfb3* deficiency lowered lactate levels and ultimately delayed pancreatic repair. Mechanistically, lactate altered macrophage phenotype during recovery after AP, by reducing the proportion of pro-inflammatory macrophages and increasing the percentage of reparative macrophages. In the indirectly co-cultured macrophage, lactate increased lactylation levels and enhanced repair gene expression. Treatment with AZD3965, a chemical inhibitor of lactate transportation, blocked the effects on lactylation and gene expression. Besides, lactate repressed the JAK2-STAT1 pathway via GPR132 receptor, thereby suppressing the expression of pro-inflammatory genes.

CONCLUSIONS: Lactate facilitates pancreatic repair by promoting reparative macrophage polarization, achieved through promoting lactylation and inhibiting JAK2-STAT1 signaling.

This phenotypic shift alleviates inflammation and facilitates tissue recovery, highlighting a potential therapeutic approach for AP. (*Cell Mol Gastroenterol Hepatol* 2025;19:101535; <https://doi.org/10.1016/j.jcmgh.2025.101535>)

Keywords: Lactate; Lactylation; Macrophage; Pancreatic Repair.

Acute pancreatitis (AP) is one of the most prevalent disorders of the digestive system. The incidence of AP is rising globally, posing a significant threat to human life and health.¹ However, current management strategies for AP remain confined to multidisciplinary approaches focused on symptomatic support, with a notable absence of targeted pharmacological treatments addressing its pathogenesis.² Clinically, 85% of cases of mild AP demonstrate the capacity for spontaneous resolution,³ indicating the presence of endogenous defense and repair mechanisms within the body.^{4,5} Incomplete pancreatic repair following AP injury will lead to impaired exocrine pancreatic function, formation of pancreatic pseudocysts, and progression to chronic pancreatitis.^{6–8} Unfortunately, the mechanisms underlying pancreatic repair and regeneration following AP remain inadequately understood. Thus, elucidating these mechanisms is crucial for gaining insights into potential clinical treatments.

Macrophages play a pivotal role in the recovery process following AP. These cells exhibit high heterogeneity and plasticity, with dynamic phenotypic changes occurring throughout the recovery process.^{9,10} In the acute injury phase, macrophages adopt a pro-inflammatory phenotype, amplifying the inflammatory response. As repair progresses, they switch to an anti-inflammatory phenotype, releasing cytokines like vascular endothelial growth factor α (VEGF α) that promote pancreatic repair.^{9–11} Studies have demonstrated that macrophage depletion during the recovery following AP significantly impairs acinar ductal metaplasia (ADM) and prolongs the resolution of inflammation.⁹ Understanding the molecular mechanisms governing macrophage polarization is essential for regulating pancreatic repair following AP.

During AP, glycolysis increases within pancreatic tissue, leading to elevated levels of the metabolite lactate.¹² Although lactate was initially regarded as a simple metabolic byproduct, it is now recognized as a key factor in signal transduction and epigenetic regulation, particularly in modulating inflammatory responses.^{13,14} Studies have shown that lactate can inhibit nucleotide-binding oligomerization domain-like receptor protein 3 (NLRP3) inflammasome activation and suppress inflammatory cytokine production through G protein-coupled receptor 81 (GPR81) activation,¹⁵ thereby mitigating inflammation in conditions such as caerulein and lipopolysaccharides (LPS) induced severe AP (SAP), autoimmune hepatitis, colitis, and rheumatoid arthritis.^{16,17} Besides, it is worth mentioning that, in the clinical treatment of AP, several studies have demonstrated that the administration of lactated Ringer's solution during fluid resuscitation results in a shorter duration of illness, fewer complications, and a lower

incidence of severe cases compared with normal saline, reflecting improved clinical outcomes.^{18–20} Additionally, the latest American College of Gastroenterology (ACG) guidelines recommend the administration of lactated Ringer's solution for moderate-intensity fluid resuscitation in patients with AP.²¹ However, the specific mechanisms underlying these benefits have not yet been fully elucidated.

Moreover, numerous studies have investigated the repair function of lactate, demonstrating that lactate can target macrophages to promote tissue repair. Lactate promotes ischemic muscle regeneration by inducing M2 macrophage polarization, and efferocytosis-induced lactate (EIL) promotes tissue repair by stimulating macrophage proliferation.^{22,23} In addition, lactate promotes histone lactylation through epigenetic regulation and enhances the expression of genes involved in wound healing in macrophages.²⁴ However, the role of lactate during the repair phase of AP remains unexplored, and whether it exerts its effects through macrophage regulation remains unclear.

This study aims to clarify the precise mechanisms by which lactate contributes to pancreatic repair after AP, offering novel mechanistic insights for AP treatment.

Results

Lactate Levels Increase During Pancreatic Repair Following AP, and Exogenous Lactate Administration Facilitates Pancreatic Recovery

Given that lactated Ringer's solution has demonstrated promising outcomes in the treatment of patients with AP,^{18–20} we aimed to further investigate the role of lactate in pancreatic repair following AP. Firstly, the cerulein-induced recovery AP (RAP) model was established (Figure 1A). Serum lactate levels in mice displayed an initial rise

*Authors share co-first authorship.

Abbreviations used in this paper: 3D, three-dimensional; ACG, American College of Gastroenterology; ADM, acinar ductal metaplasia; ANOVA, analysis of variance; AP, acute pancreatitis; cDNA, complementary DNA; Ck19, cytokeratin 19; CM, culture media; D0, day 0; D1, day 1; D3, day 3; DAMP, damage-associated molecular pattern; DAPI, 4',6-diamidino-2-phenylindole; DMEM, Dulbecco's Modified Eagle Medium; EIL, efferocytosis-induced lactate; ELISA, enzyme-linked immunosorbent assay; FACS, fluorescence-activated cell sorting; FBS, fetal bovine serum; FITC, fluorescein isothiocyanate; GO, gene ontology; GPR81, G protein-coupled receptor 81; H&E, hematoxylin and eosin; IL1 β , interleukin 1 β ; IL6, interleukin 6; IP, immunoprecipitation; KEGG, Kyoto Encyclopedia of Genes and Genomes; Lac, lactate; LPS, lipopolysaccharides; MCT1, monocarboxylate transporter 1; NLRP3, nucleotide-binding oligomerization domain-like receptor protein 3; PAC, pancreatic acinar cell; PBS, phosphate buffered saline; Pfkfb3, 6-Phosphofructo-2-Kinase/Fructose-2,6-Biphosphatase 3; RAP, recovery AP; Rplp0, Ribosomal protein lateral handle subunit P0; RT-qPCR, reverse transcription quantitative polymerase chain reaction; SAP, severe acute pancreatitis; SDS-PAGE, sodium dodecyl sulfate-polyacrylamide gel electrophoresis; SEM, standard error of the mean; Sox9, SRY-Box Transcription Factor 9; Tnfa, tumor necrosis factor α ; VEGF α , vascular endothelial growth factor α ; WB, Western blot; WT, wild-type.

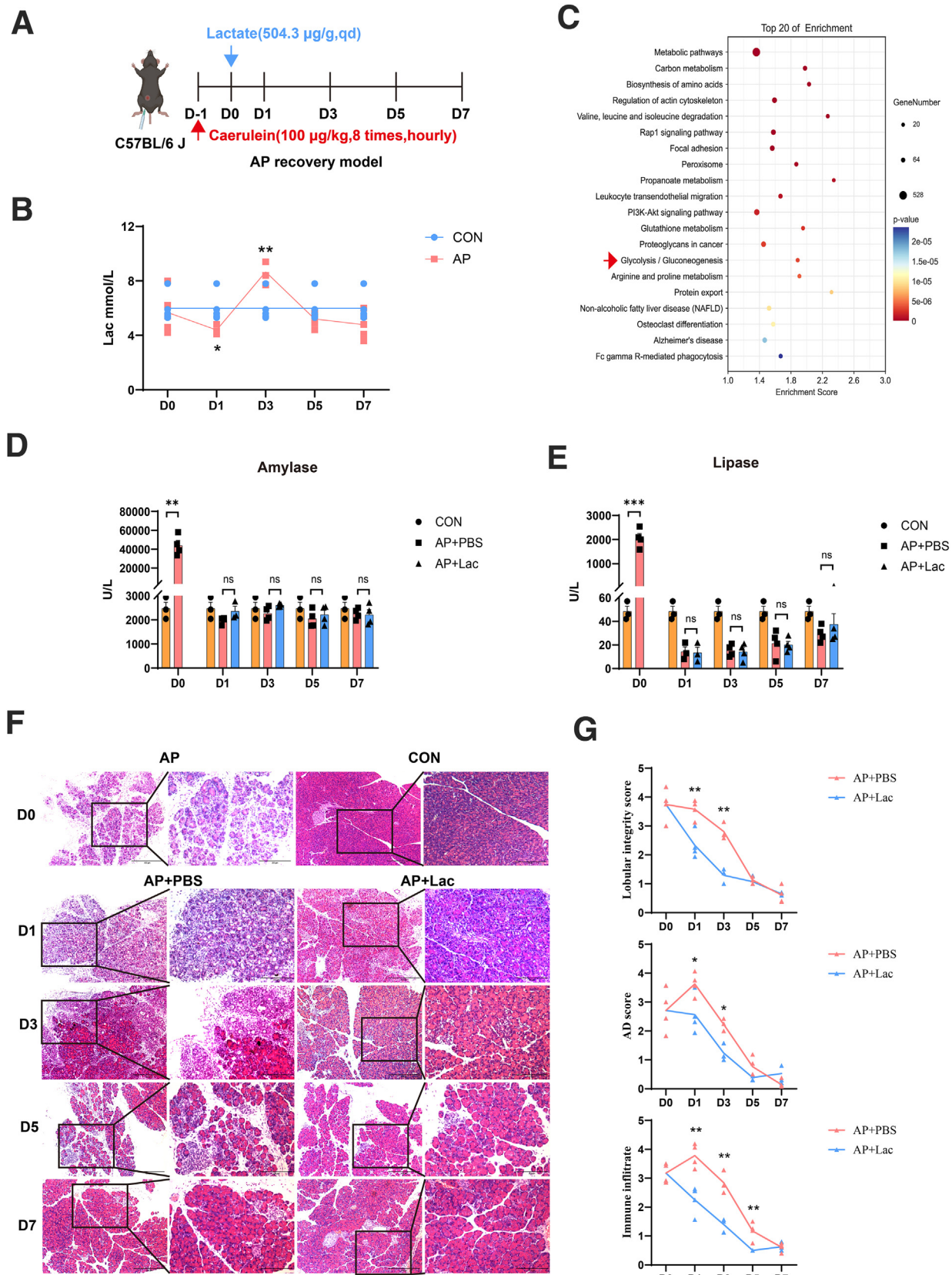


Most current article

© 2025 The Authors. Published by Elsevier Inc. on behalf of the AGA Institute. This is an open access article under the CC BY-NC-ND license (<http://creativecommons.org/licenses/by-nc-nd/4.0/>).

2352-345X

<https://doi.org/10.1016/j.jcmgh.2025.101535>



followed by a decline (Figure 1B) during pancreatic repair after AP. Besides, through RNA sequencing and Kyoto Encyclopedia of Genes and Genomes (KEGG) enrichment pathway analysis,²⁵ it was found that the glycolysis/gluconeogenesis pathway in the pancreas was significantly upregulated during cerulein-induced AP (Figure 1C), which indicated the elevated level of metabolite lactate. The elevated lactate level indicates that lactate may play a crucial role in pancreatic repair following AP. Furthermore, after the cerulein-induced RAP model was established, an exogenous lactate was administrated, and pancreatic tissue and serum samples were collected at different time points over the course of 1 week (Figure 1A). Elevated serum amylase and lipase levels are closely associated with acinar injury and necrosis in cerulein-induced AP. It was discovered that the serum levels of amylase and lipase in mice were significantly elevated on day 0 (D0) (Figure 1D–E), whereas at subsequent time points, serum levels of amylase and lipase were reduced to normal (Figure 1D–E), indicating the initiation of the pancreatic repair phase. Additionally, compared with the AP + phosphate buffered saline (PBS) group, the lactate administration group exhibited improved lobular integrity in pancreatic tissue, with fewer dedifferentiated acinar cells and inflammatory cells (Figure 1F–G), particularly on days 1 (D1) and 3 (D3).

Furthermore, lactate administration did not adversely affect the morphology or function (Figure 2A–C) of pancreas in healthy mice. Subsequently, amylase expression in pancreatic tissue was detected to evaluate acinar integrity. It was found that amylase levels in the lactate administration group were significantly elevated compared with the control group (Figure 2D–E), suggesting that lactate mitigates damage and facilitates repair during the recovery following AP. Taken together, lactate levels increase during pancreatic repair following AP, and exogenous lactate administration promotes pancreatic recovery.

6-Phosphofructo-2-Kinase/Fructose-2,6-Biphosphatase 3 Deficiency Reduces Lactate Levels and Delays Pancreatic Repair Following AP

Next, we aimed to investigate the effect of low lactate levels on pancreatic repair and to further elucidate the role of lactate in this process. Lactate production is closely associated with the glycolysis pathway,¹³ which is affected by the key enzyme 6-Phosphofructo-2-Kinase/Fructose-2,6-Biphosphatase 3 (Pfkfb3).²⁶ Pfkfb3 deficiency results in downregulation of glycolysis, ultimately

leading to reduced lactate production.²³ Furthermore, the transcriptional level of *Pfkfb3* was significantly upregulated during cerulein-induced AP (Figure 3A), and its expression levels fluctuated dynamically during the recovery of post-AP (Figure 3B). These data suggest that Pfkfb3 may influence pancreatic repair by modulating lactate levels. Thus, heterozygous *Pfkfb3* mice were used in this study because homozygous knockout of this gene results in lethality.²⁷ It was observed that, compared with wild-type (WT) mice, serum lactate levels in heterozygous mice were significantly decreased (Figure 3C). Additionally, both Pfkfb3 mRNA and protein levels in pancreatic tissue were markedly reduced (Figure 3D–E). Moreover, the deficiency did not affect pancreatic tissue morphology, the expression of inflammatory factors interleukin 6 (Il6), interleukin 1 β (Il1 β), tumor necrosis factor α (Tnf α) in serum, or the levels of amylase and lipase (Figure 3F–I).

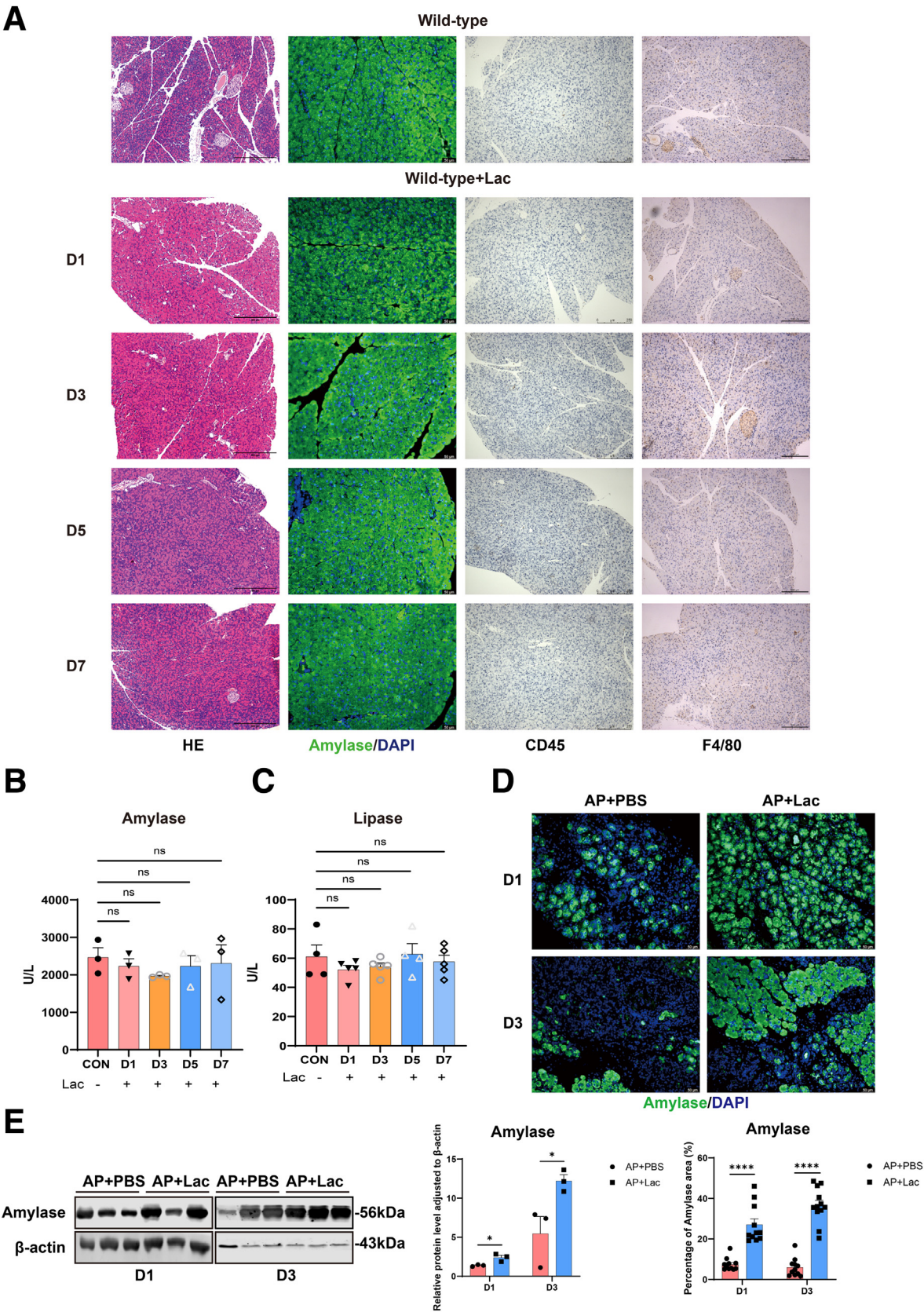
Subsequently, these mice were utilized to establish the RAP model. Specially, serum lactate levels in *Pfkfb3* deficiency mice were markedly reduced compared with those in WT mice on D1 and D3 (Figure 4A). Besides, the *Pfkfb3*^{+/-} mice exhibited impaired pancreatic integrity, elevated levels of ADM, and increased inflammatory cell infiltration (Figure 4B–C). Additionally, *Pfkfb3* deficiency significantly increased the expression levels of inflammatory genes *Il6*, *Il1 β* , and *Tnf α* in pancreatic tissue (Figure 4D), as well as the levels of inflammatory factors, amylase, and lipase in serum (Figure 4E–G). These results indicate that the deficiency of *Pfkfb3* reduces lactate levels, ultimately delaying pancreatic repair following AP.

Lactate Promotes Pancreatic Repair Following AP by Improving Inflammatory Immune Microenvironment

Given the critical role of the inflammatory response in recovery following AP, and because lactate has been shown to alleviate cerulein- and LPS-induced SAP,¹⁷ we hypothesized that lactate promotes pancreatic repair by modulating inflammation. First, CD45 and F4/80 expression levels (Figure 5A–B) were measured in pancreatic tissue on D1 and D3. It was observed that, compared with the control group, leukocyte and macrophage numbers in the lactate administration group were significantly reduced. Furthermore, a significant reduction was found in the expression of inflammatory factors in both pancreatic tissue (Figure 5C) and serum (Figure 5D).

Figure 1. (See previous page). Lactate levels increase during pancreatic repair following AP and exogenous lactate administration facilitates pancreatic recovery. (A) A schematic diagram illustrating the construction of the RAP model and the timeline for lactate administration. Mice were sacrificed on day 0, 1, 3, 5, and 7 following AP induction. **(B)** Serum lactate levels in mice at different time points during recovery following AP, $n = 3$ –5/group. **(C)** Transcriptome sequencing of pancreatic tissue from WT mice subjected to cerulein-induced AP, followed by KEGG pathway analysis of significantly differentially expressed genes, $n = 6$ /group. **(D–E)** Serum amylase (D) and lipase (E) levels were measured during recovery following AP, $n = 3$ –4/group. **(F–G)** Histologic alterations in the pancreatic tissue of mice were analyzed using H&E staining (F). Scores for lobular integrity, acinar dedifferentiation, and inflammatory cell infiltration were quantified (G). The zoomed-in images represent high-magnification views of the outlined areas, with scale bars representing 400 μ m and 200 μ m, $n = 3$ –4/group. Data are expressed as mean \pm SEM. Statistical significance is indicated as follows: ns means $P > .05$, * $P < .05$; ** $P < .01$; and *** $P < .001$.

Besides, pancreatic acinar cell proliferation and ADM resolution are 2 key processes required for complete pancreatic regeneration.^{28,29} Primary acinar cell 3-dimensional (3D) culture is a well-established model for evaluating ADM.³⁰⁻³² To explore the effect of lactate on ADM during pancreatic repair following AP, primary acinar cell



3D culture technology was employed. Our data showed that exogenous lactate intervention did not significantly alter the number of ductal cells (Figure 6A), nor did it affect the expression of ductal cell markers (cytokeratin 19 [Ck19]) or cell proliferation ability (Figure 6B–E), indicating that lactate had no significant effect on ADM and acinar proliferation during pancreatic regeneration.

Specifically, due to the powerful effect of lactate in alleviating inflammation during pancreatic repair, it ultimately enables pancreatic tissue to achieve homeostasis more rapidly. This phenomenon was accompanied by a reduced proportion of ductal cell markers (Ck19, SRY-Box Transcription Factor 9 [Sox9]) and increased Ki67 expression levels (Figure 7A–C). In addition, lactate intervention in normal mice did not affect the expression levels of ductal cell markers (Ck19, Sox9) or Ki67 (Figure 7A–C). Collectively, these findings suggest that lactate promotes pancreatic repair following AP by improving inflammatory immune microenvironment.

Lactate Promotes Reparative Macrophage Polarization During the Recovery Following AP

Based on the role of lactate in mitigating inflammation during AP repair, we subsequently focused on immune cells. Macrophages are a type of widely distributed and functionally diverse immune cells. Previous studies have demonstrated that they play a critical role in pancreatic repair following AP.^{9–11} Therefore, we wondered whether lactate promotes pancreatic repair by regulating the phenotype and function of macrophages. First, macrophages were isolated from the pancreas of mice at different time points, using fluorescence-activated cell sorting (FACS) (Figure 8A), followed by micro-transcriptome sequencing. The sequencing data showed that after lactate administration, the expression of pro-inflammatory genes such as *Csf1*, *Thbs1*, *Ccl17*, and *Cxcl10* in macrophages was significantly reduced, whereas repair genes like *Ccnd1*, *Vefgc*, *Cdc20*, and *Ccnb1* were upregulated (Figure 8B–D). Moreover, gene ontology (GO) analysis indicated that on D1, compared with the control group, anti-inflammatory and angiogenesis-related pathways in the lactate administration group were distinctly upregulated, whereas immune response and inflammatory response-related pathways were significantly downregulated (Figure 8E). Similarly, after lactate intervention, pathways associated with cell proliferation were significantly upregulated, whereas pathways associated with pro-inflammatory responses were downregulated on D3 (Figure 8F). Therefore, these data suggested that lactate

intervention induced significant changes in the macrophage transcriptome, notably enhancing the expression of genes associated with reparative macrophages.

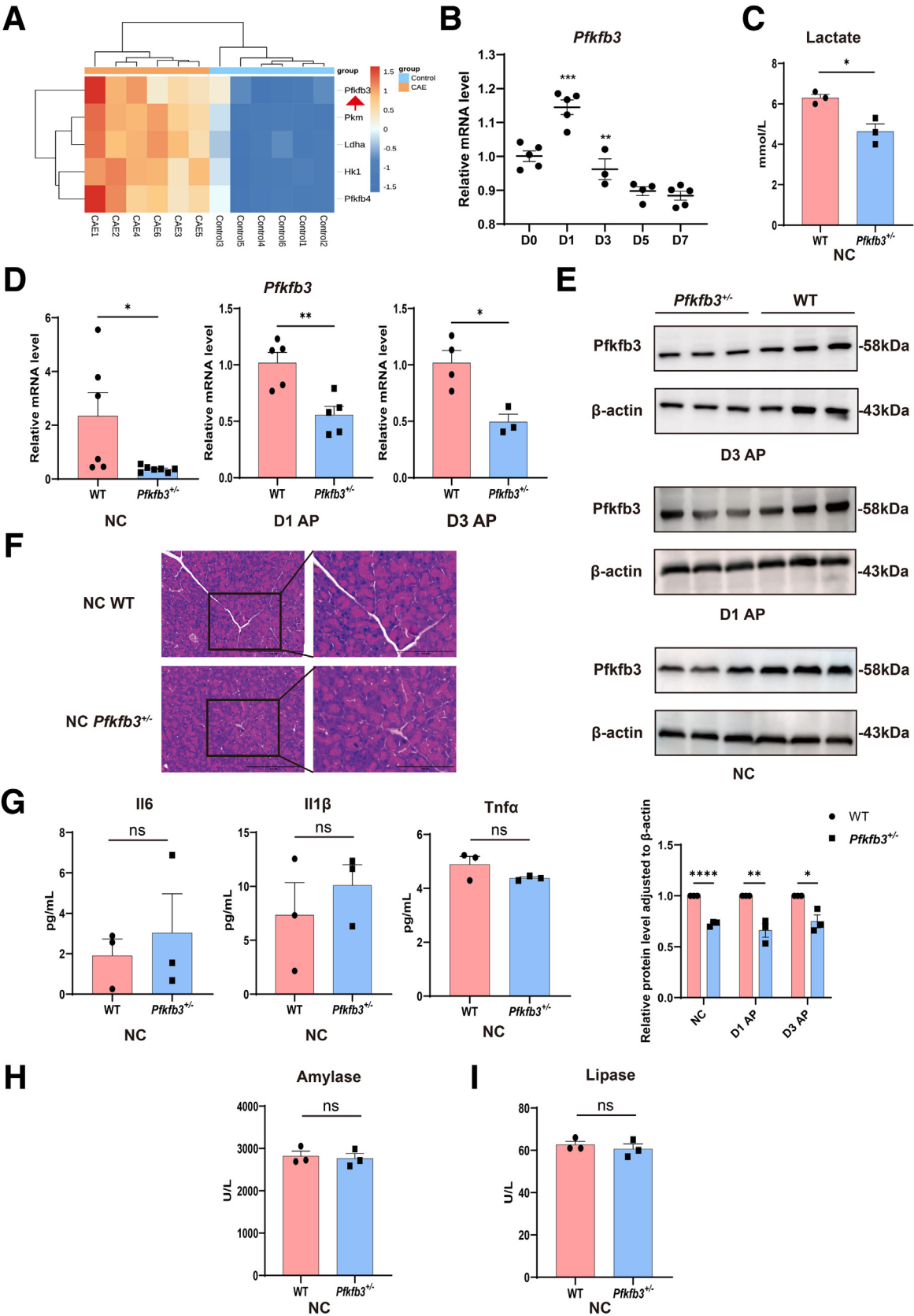
Subsequently, histologic analyses were performed to further validate the observed phenomenon. Flow cytometry analysis revealed that during the pancreatic repair after AP, lactate treatment significantly decreased the proportion of pro-inflammatory macrophages (iNOS⁺, CD86⁺), whereas it increased the percentage of reparative macrophages (Arg1⁺, CD206⁺) (Figure 9A–B). Additionally, the immunofluorescence analysis results were consistent with the flow cytometry data, demonstrating a decrease in the proportion of F4/80⁺iNOS⁺ cells and an increase in F4/80⁺CD206⁺ cells following lactate administration on D1 and D3 (Figure 9C–D). Collectively, the above results indicated that lactate modulates the polarization of macrophages during pancreatic repair following AP, promoting the switch from pro-inflammatory macrophages to reparative macrophages and ultimately supporting pancreatic tissue recovery.

Lactate Increases Lactylation Level via Monocarboxylate Transporter 1 to Regulate Macrophage Polarization

We next aimed to explore the mechanisms by which lactate regulates macrophage polarization. Studies have reported that lactylation alters macrophage phenotypes and functions.^{24,33} Lactate was shown to act as a precursor for the lactylation of histone lysine residues.²⁴ Therefore, we wondered whether the regulation of macrophage polarization by lactate during recovery following AP may also be mediated by lactylation. To this end, macrophage lactylation levels in pancreatic tissue were first examined, revealing that, after lactate treatment, macrophage lactylation levels were significantly elevated on D1 and D3 (Figure 10A). These data suggest that elevated level of macrophage lactylation induced by lactate may play a critical role in pancreatic repair following AP.

Subsequently, we tested it in ex vivo. Macrophage activation during pancreatitis was simulated by indirectly co-culturing inflammatory acinar cells and macrophages (Figure 10B), revealing an increase in intracellular lactate levels upon macrophage activation (Figure 10C). Previous studies have reported that monocarboxylate transporter 1 (MCT1) is a key transport protein of lactate.^{34,35} Thus, we wondered whether lactate enters cell through MCT1. By measuring the lactate level in indirectly co-cultured macrophages, it was discovered that lactate levels significantly increased after lactate administration, whereas this effect

Figure 2. (See previous page). Lactate administration does not impact pancreatic morphology or function in healthy mice. (A) H&E staining was performed to evaluate the morphologic effects of lactate administration on pancreatic tissue, scale bar = 400 μ m. Immunofluorescence was utilized to assess the expression of amylase (green) in pancreatic tissue, DAPI (blue), scale bar = 50 μ m. Immunohistochemistry was conducted to evaluate the expression of CD45⁺ and F4/80⁺ cells in pancreatic tissue, scale bars = 250 μ m, 200 μ m, n = 5/group. (B–C) Lactate administration did not significantly influence the expression levels of serum amylase (B) and lipase (C) in healthy mice, n = 3–5/group. (D) Representative images and relative quantification of pancreatic amylase expression were assessed via immunofluorescence staining. Amylase (green), DAPI (blue), scale bar = 50 μ m, n = 11–12/group. (E) WB analysis of amylase expression level in pancreatic tissue during recovery following AP, n = 3/group. Data are expressed as mean \pm SEM. Statistical significance is indicated as follows: ns means $P > .05$; * $P < .05$; and *** $P < .0001$.



was reversed by the addition of the MCT1 inhibitor AZD3965 (Figure 10C), confirming that lactate influx in macrophages occurs via MCT1. Besides, AZD3965 intervention significantly reduced the level of extracellular lactate in indirectly co-cultured macrophages (Figure 10D). Next, the lactylation level in indirectly co-cultured macrophages was evaluated by immunofluorescence, and we found that lactylation levels increased following lactate intervention but were reversed by AZD3965 (Figure 10E).

Based on the above results, immunoprecipitation (IP) was performed to identify lactylated proteins in indirectly co-cultured macrophages, aiming to identify the downstream targets of lactate. Notably, 162 proteins exhibited upregulated lactylation levels following lactate intervention, and these proteins are associated with pathways related to glycolysis, pyruvate metabolism, and lactate production (Figure 10F–G). Additionally, 153 proteins displayed downregulated lactylation levels after AZD3965 treatment, primarily associated with the ribosomal pathways (Figure 10H–I).

Among all proteins with increased lactylation levels after lactate treatment, the most representative ones were histone H3, histone H4, Hmgb1, and Ldha (Figure 11A). Then, these findings were validated through IP, which confirmed that histone H3, histone H4, Hmgb1, and Ldha were lactylated, with their levels increasing following lactate administration; however, this effect was weakened after AZD3965 intervention (Figure 11B–C). Additionally, consistent results were obtained by Western blot (WB) analysis using an antibody against histone H3 K18 lactylation (Figure 11D). These data indicated that lactate enters AP-activated macrophages via MCT1, promoting histone H3, histone H4, Hmgb1, and Ldha lactylation.

Previous studies have demonstrated that histone lactylation regulates gene expression.^{36–39} Gene expression in indirectly co-cultured macrophages was subsequently examined after histone lactylation, revealing that lactate intervention reduced the expression of pro-inflammatory genes (*Tnfα*, *Il-6*, *Nos2*) and increased the expression of repair genes (*Lrg1*, *Vegfa*, *Retnla*). This effect was reversed by the addition of the MCT1 inhibitor AZD3965 (Figure 11E–F).

Together, these results indicated that lactate promotes lactylation through MCT1, facilitating the transition of macrophages from a pro-inflammatory phenotype to a reparative phenotype.

Lactate Inhibits the JAK2-STAT1 Signaling Pathway in Macrophages Through the GPR132 Receptor, Facilitating a Switch in Macrophage Phenotype

By transcriptome sequencing, it was found that lactate significantly inhibited the JAK-STAT signaling pathway in macrophage during the recovery following AP (Figure 12A). Earlier studies have demonstrated that this signaling pathway is closely related to the initiation and development of various inflammatory diseases.^{40,41} Among these, the JAK-STAT3 pathway is involved in the production of pro-inflammatory cytokines in SAP,^{42,43} thereby regulating its degree of inflammation. Additionally, the JAK-STAT1 pathway is closely associated with M1-like macrophage polarization and the production of pro-inflammatory cytokines.^{40,44} Subsequently, we aim to investigate the mechanisms by which lactate regulates the JAK-STAT signaling pathway and examine its association with macrophage phenotypes.

The GPR132 receptor is a G protein-coupled receptor located on the macrophage membrane that can sense lactate signals, mediating the effect of lactate in regulating tumor-associated M2 macrophages.⁴⁵ Studies have indicated that G protein-coupled receptors can activate STAT3 by stimulating JAK2.⁴⁶ Therefore, we wonder whether lactate regulated the JAK2-STAT1 signaling pathway through the GPR132 receptor. Firstly, lactate was found to significantly reduce GPR132 mRNA levels in macrophages during pancreatic repair after AP (Figure 12A). Besides, in ex vivo, the mRNA level of GPR132 in indirectly co-cultured macrophages was reduced by lactate, which was reversed by the addition of a GPR132 antagonist (Figure 12B). Furthermore, our experimental results demonstrated that the JAK2-STAT1 pathway was activated during the activation of indirectly co-cultured macrophages, whereas this signaling was significantly inhibited after lactate intervention. In contrast, the inhibitory effect by lactate was reversed upon the addition of the GPR132 antagonist (Figure 12C–D). These results suggested that lactate inhibits the JAK2-STAT1 pathway via the GPR132 receptor.

Next, the correlation between the JAK2-STAT1 pathway and macrophage phenotypes was explored. Reverse transcription quantitative polymerase chain reaction (RT-qPCR) results showed that following inhibition of the JAK2-STAT1 pathway, the expressions of pro-inflammatory genes such as *Cxcl10*, *Ccl12*, and *Il6* were significantly downregulated

Figure 3. (See previous page). *Pfkfb3* deficiency reduces lactate levels without affecting pancreatic morphology or function in healthy mice. (A) Transcriptome sequencing of pancreatic tissue from WT mice during cerulein-induced AP, presented as a heatmap of differentially expressed genes associated with the glycolysis pathway, $n = 6/\text{group}$. (B) *Pfkfb3* mRNA expression level during recovery following AP was determined by qPCR, $n = 3\text{--}5/\text{group}$. (C) Serum lactate levels in heterozygous *Pfkfb3* mice, $n = 3\text{--}5/\text{group}$. (D–E) The efficiency of *Pfkfb3* deficiency was determined by qPCR in the pancreatic tissue of *Pfkfb3*^{+/-} mice (D), WB analysis confirmed protein deficiency efficiency (E), and a relative quantification graph is presented, $n = 3\text{--}7/\text{group}$. (F) Histologic alterations in *Pfkfb3*^{+/-} mouse pancreas were analyzed by H&E staining. The zoomed-in images represent high-magnification views of the outlined areas, with scale bars representing 400 μm and 200 μm , $n = 3/\text{group}$. (G) Serum levels of inflammatory factors were evaluated in healthy mice following *Pfkfb3* deficiency, $n = 3/\text{group}$. (H–I) Serum amylase (H) and lipase (I) levels in *Pfkfb3*^{+/-} mice and WT mice, $n = 3\text{--}7/\text{group}$. Data are expressed as mean \pm SEM. Statistical significance is indicated as follows: ns means $P > .05$; * $P < .05$; ** $P < .01$; *** $P < .001$; and **** $P < .0001$.

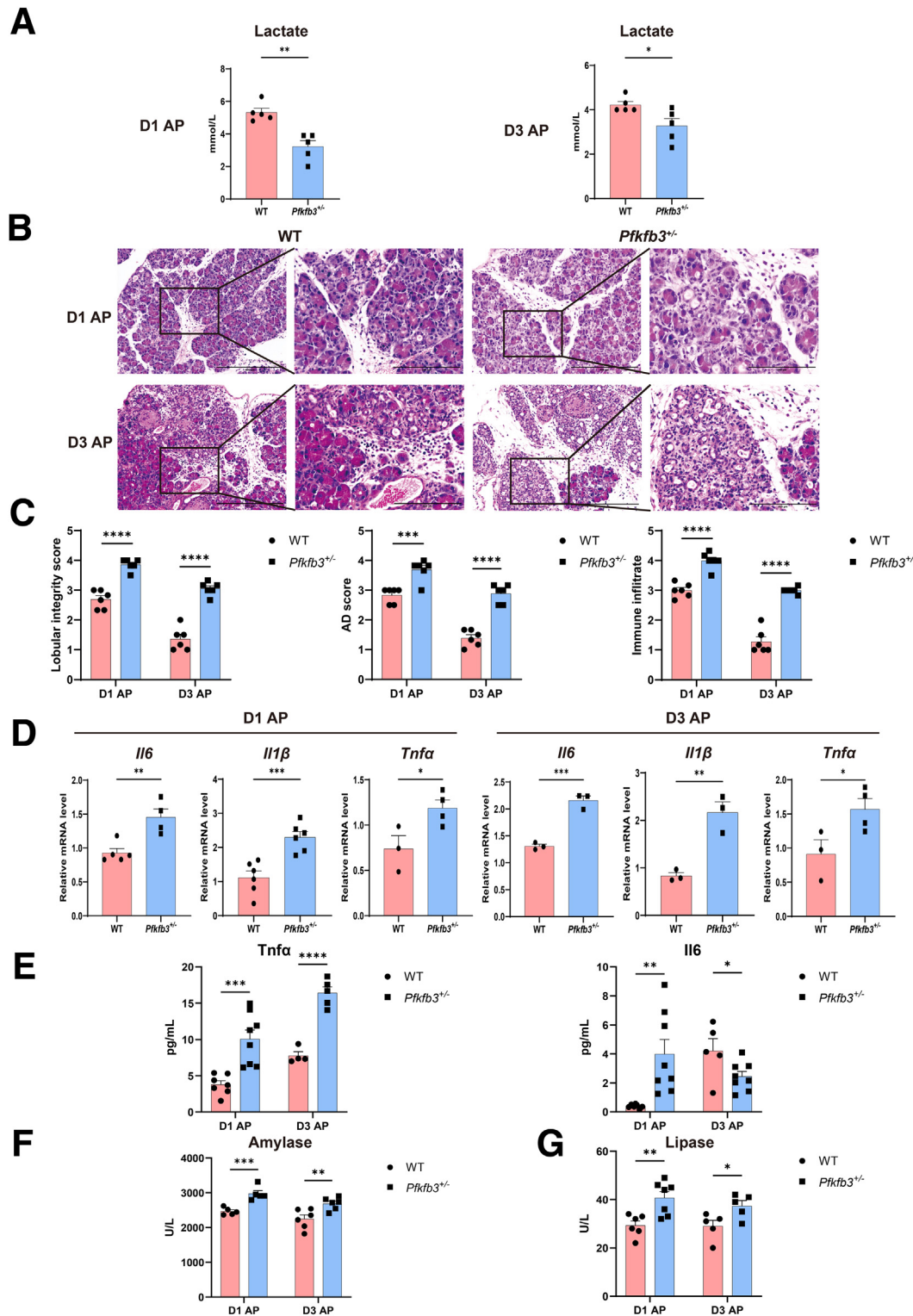


Figure 4. *Pfkfb3* deficiency delays pancreatic repair following AP. (A) Serum lactate levels in WT mice and *Pfkfb3*^{+/-} mice in the RAP model, n = 3–5/group. (B–C) Histologic alterations in the pancreatic tissue of mice were assessed using H&E staining (B). Quantitative scores for lobular integrity, acinar dedifferentiation, and inflammatory cell infiltration were recorded (C). The zoomed-in images represent high-magnification views of the outlined areas, with scale bars representing 400 μ m and 200 μ m, n = 6/group. (D) qPCR analysis of inflammatory factor expression levels in pancreatic tissue on D1 and D3 in the RAP model, n = 3–6/group. (E) ELISA was employed to measure serum levels of the inflammatory factors *Tnfa* and *Il6* on D1 and D3 during recovery following AP, n = 4–8/group. (F–G) Serum amylase (F) and lipase (G) levels in WT mice and *Pfkfb3*^{+/-} mice in the RAP model, n = 5–6/group. Data are expressed as mean \pm SEM. Statistical significance is indicated as follows: **P* < .05; ***P* < .01; ****P* < .001; and *****P* < .0001.

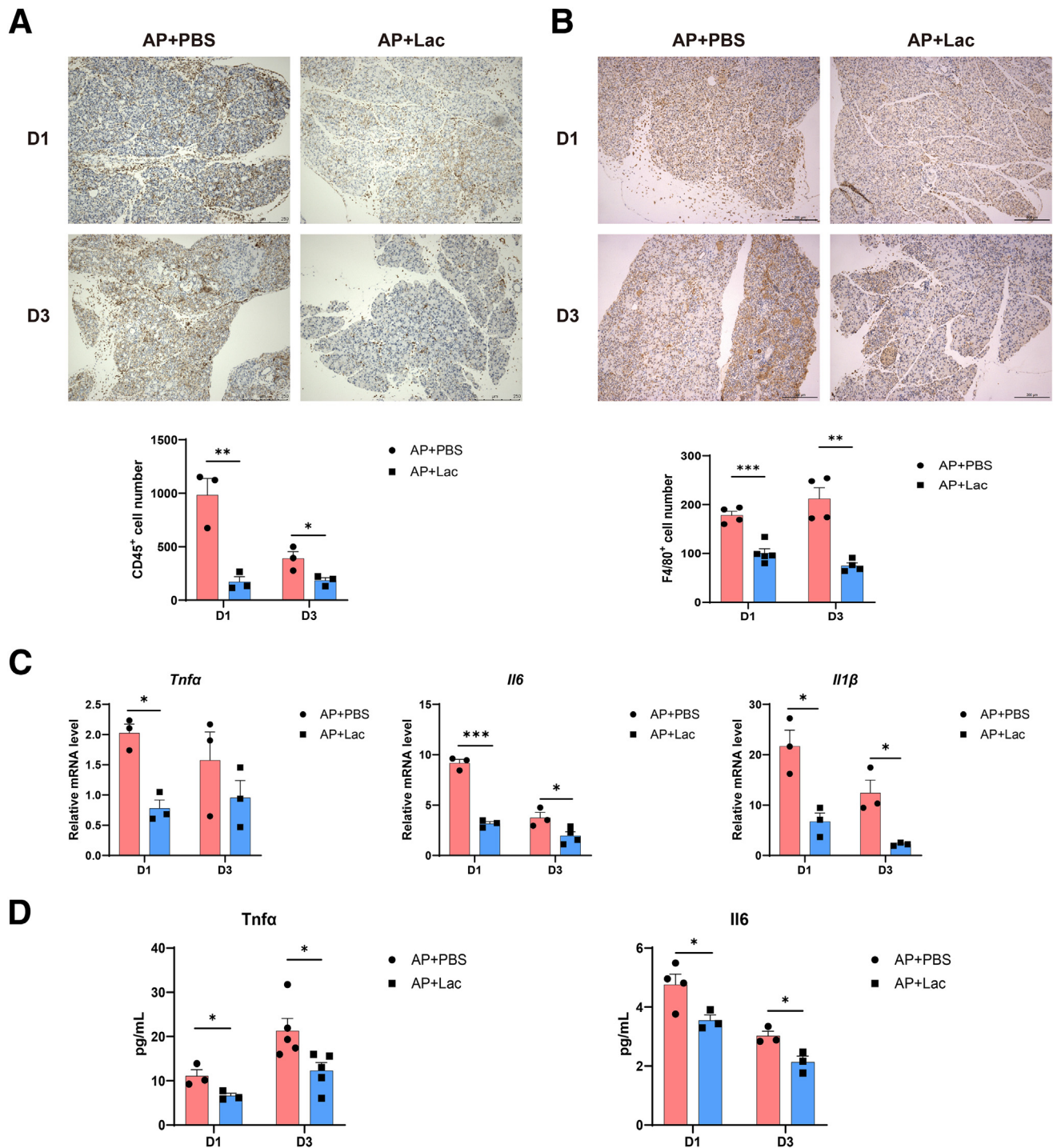


Figure 5. Lactate promotes pancreatic repair following AP by improving inflammatory immune microenvironment. (A) Representative images illustrating CD45 expression in pancreatic tissue on D1 and D3 during recovery following AP, evaluated by immunohistochemistry. CD45 intensity was quantified. Scale bar = 250 μ m, positive areas were marked and counted using Image J software, $n = 3$ /group. (B) Representative images depicting F4/80 expression in pancreatic tissue on D1 and D3 during recovery following AP, assessed through immunohistochemistry, along with corresponding quantification images. Scale bar = 250 μ m; positive areas were marked and counted using Image J software, $n = 4-5$ /group. (C) Expression levels of inflammatory factors *Tnfa*, *Il6*, and *Il1β* in pancreatic tissue on D1 and D3 were quantified by qPCR, $n = 3-4$ /group. (D) Serum levels of the inflammatory factors *Tnfa* and *Il6* on D1 and D3 in mice were measured using ELISA, $n = 3-5$ /group. Data are expressed as mean \pm SEM. Statistical significance is indicated as follows: * $P < .05$; ** $P < .01$; and *** $P < .001$.

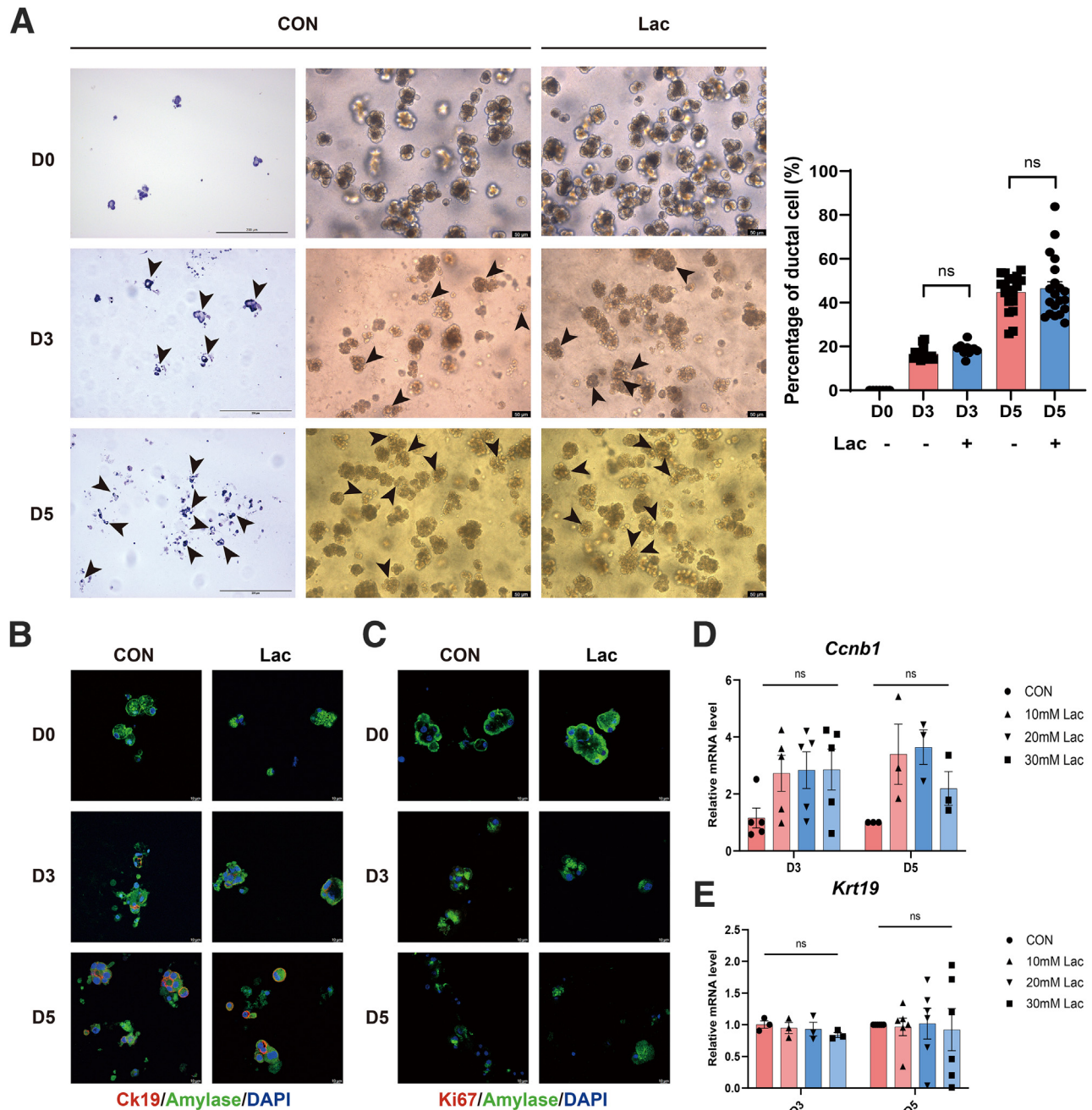


Figure 6. Lactate had no significant impact on ADM or acinar proliferation during pancreatic regeneration. (A) Representative images of primary acinar cell 3D culture, accompanied by H&E staining and quantitative analysis, $n = 7\text{--}20/\text{group}$. (B) Immunofluorescence assessment of Ck19 (red) and Amylase (green) co-localization during the 3D culture of primary acinar cells, DAPI (blue), scale bar = $10\text{ }\mu\text{m}$. (C) The co-localization of Ki67 (red) and Amylase (green) during the 3D culture of primary acinar cells was examined through immunofluorescence, DAPI (blue), scale bar = $10\text{ }\mu\text{m}$. (D) The expression levels of *Ccnb1* in primary acinar cells during 3D culture were determined using qPCR, $n = 3\text{--}5/\text{group}$. (E) The expression levels of *Krt19* in primary acinar cells during 3D culture were assessed by qPCR, $n = 3\text{--}6/\text{group}$. Data are expressed as mean \pm SEM. Statistical significance is indicated as follows: ns means $P > .05$.

(Figure 12E), whereas the expressions of repair genes like *Lrg1*, *Retnla*, and *Vegfa* were significantly upregulated (Figure 12F). Taken together, lactate suppresses the JAK2-STAT1 signaling pathway via the GPR132 receptor, promoting the polarization of reparative macrophages.

Discussion

Lactate was traditionally regarded as a metabolic waste product; however, accumulating evidence highlights its important role in various diseases. In this study, it was observed that serum lactate levels in mice were elevated

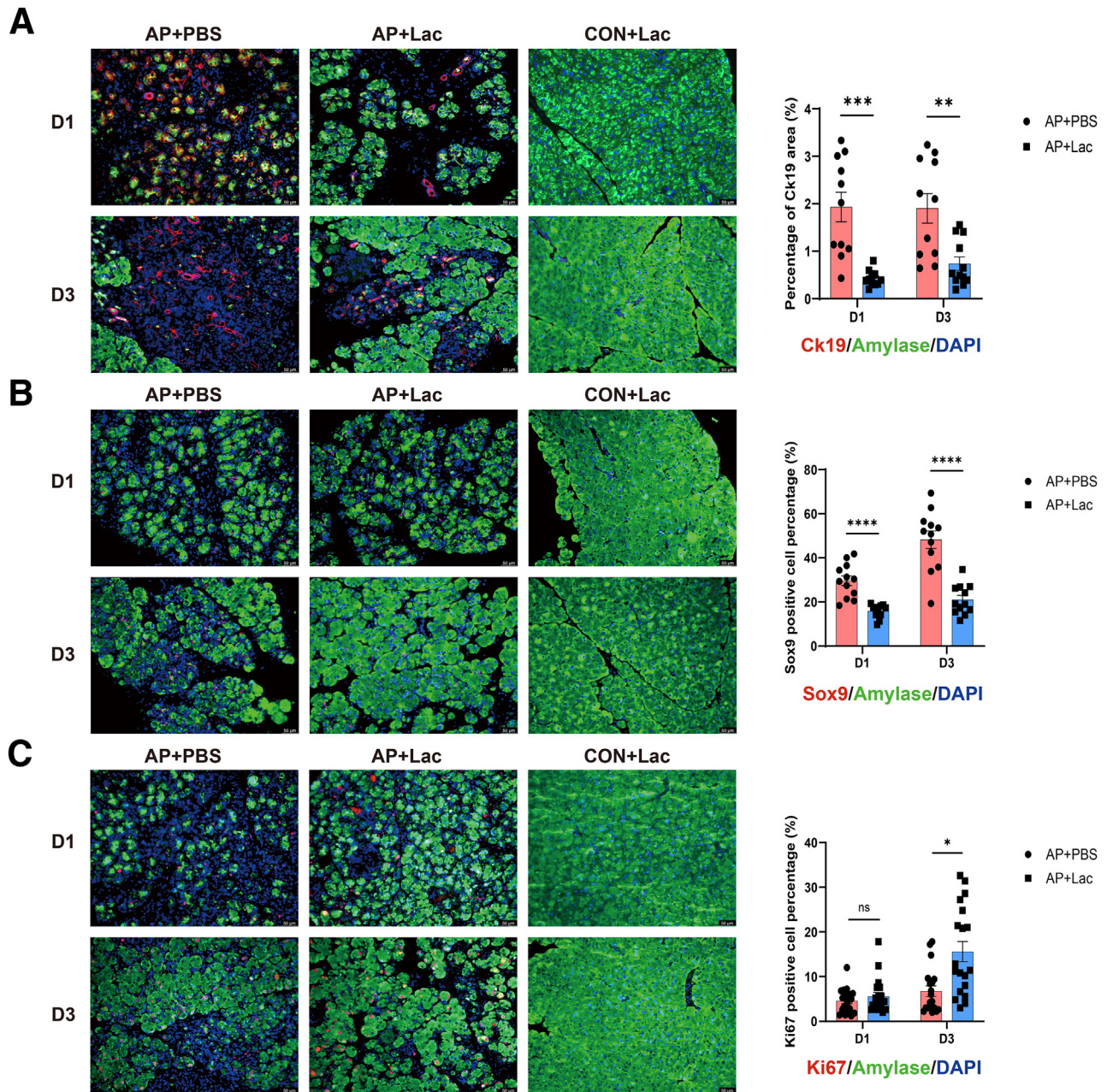
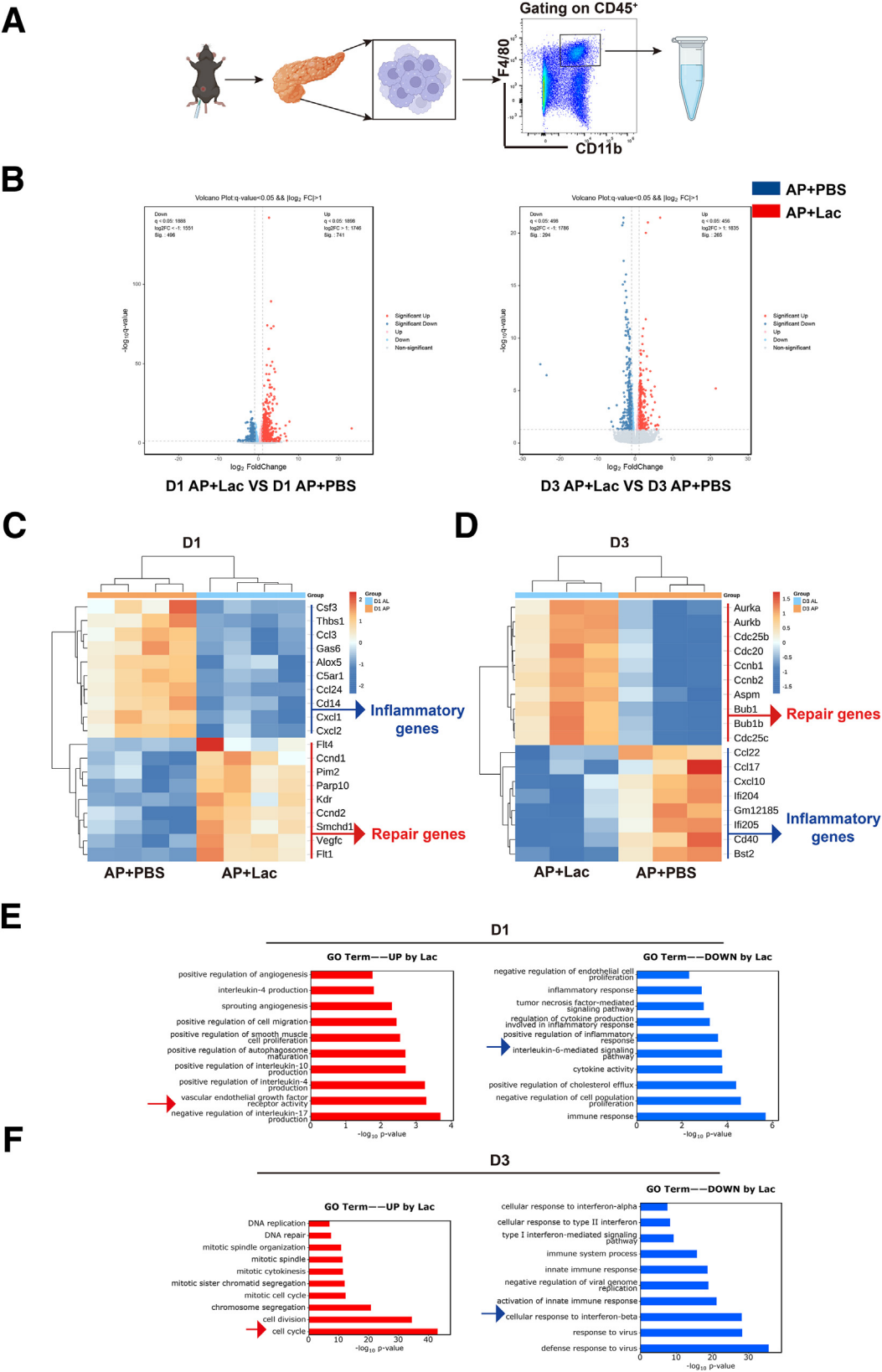


Figure 7. Lactate induces concomitant changes in ductal cells and cell proliferation markers during pancreatic repair following AP. (A) Immunofluorescence was performed to evaluate the co-localization of Ck19 (red) and Amylase (green) in pancreatic tissue during the repair process following AP, accompanied by a relative quantitative graph. DAPI (blue), scale bar = 50 μ m, n = 11–12/group. (B) Co-localization of Sox9 (red) and Amylase (green) in pancreatic tissue was assessed by immunofluorescence. DAPI (blue), scale bar = 50 μ m, n = 12/group. (C) The co-localization of Ki67 (red) and Amylase (green) in pancreatic tissue was evaluated via immunofluorescence, DAPI (blue), scale bar = 50 μ m, n = 19/group. Data are expressed as mean \pm SEM. Statistical significance is indicated as follows: ns means $P > .05$; * $P < .05$; ** $P < .01$; *** $P < .001$; and **** $P < .0001$.

during pancreatic repair after AP. Furthermore, exogenous lactate treatment significantly facilitated pancreatic repair, whereas deficiency of *Pfkfb3* genes reduced lactate levels and notably delayed pancreatic repair. These results suggest that lactate plays a crucial role in pancreatic repair following AP.

In the cerulein-induced RAP model, pancreatic repair following AP involves 3 critical processes: the resolution of inflammation, the dedifferentiation and subsequent redifferentiation of acinar cells, and the proliferation of remaining acinar cells.^{28,47} An imbalance in any of these processes will result in persistent inflammation, acinar

dedifferentiation, and fibrosis of the pancreas, ultimately impairing the repair of pancreatic tissue and potentially leading to chronic pancreatitis.²⁸ This study highlights the beneficial effect of lactate on pancreatic repair after AP, particularly its role in attenuating inflammation. Besides, our experimental data suggested that lactate did not



significantly influence the dedifferentiation and proliferation capacities of acinar cells during the recovery after AP. Thus, lactate's regulatory effect on the inflammatory immune microenvironment influences the repair process of pancreas following AP.

Additionally, this study highlights that lactate exerts its regulatory effect on the inflammatory immune microenvironment primarily by modulating macrophage phenotype. Lactate significantly decreased the percentage of pro-inflammatory macrophages, while it simultaneously increased the percentage of reparative macrophages during recovery following AP. The increased polarization of reparative macrophages contributes to the formation of an immune microenvironment conducive to tissue repair, thereby alleviating inflammation and promoting pancreatic recovery.

Furthermore, the mechanisms by which lactate regulates macrophage phenotypes were explored, in which lactylation plays a key role. Lactylation is an emerging form of post-translational modification characterized by the covalent attachment of lactate molecules to the lysine residues of proteins. This modification can influence the transcription of key genes, thereby regulating disease processes, including inflammation and cancer.⁴⁸ It was demonstrated that lactate promoted lactylation of histone H3, histone H4, *Ldha*, and *Hmgb1* in indirectly co-cultured macrophages through the lactate transporter MCT1. This modification contributed to a decrease in the expression of pro-inflammatory genes and an increase in the expression of repair genes, facilitating the switch to reparative macrophages. Consequently, the transition improves the immune microenvironment and ultimately promotes pancreatic repair following AP.

Lactate not only increased the lactylation levels of histone H3 in indirectly co-cultured macrophages, but also elevated lactylation levels of histone H4, *Ldha*, and *Hmgb1*. Histone H4, a member of the histone family, has been reported to regulate glycolytic levels in microglia through lactylation.⁴⁹ *Ldha* is an enzyme involved in lactate production during glycolysis, and its function following lactylation remains incompletely understood. *Hmgb1*, a prototypical damage-associated molecular pattern (DAMP), plays a critical role in macrophage activation, and studies suggest that its lactylation modification may enhance the recruitment and activation of macrophages.⁵⁰ However, the role of lactylation in these proteins within macrophages, particularly in the context of AP, requires further investigation.

The JAK-STAT signaling pathway is closely linked to the polarization of pro-inflammatory macrophages, with the

activation of STAT1 enhancing the transcription levels of pro-inflammatory genes, which, in turn, positively feeds back into the polarization of these macrophages.^{40,44} However, in the context of AP, lactate inhibits the JAK2-STAT1 signaling pathway via the GPR132 receptor, thereby downregulating the expression of pro-inflammatory genes while increasing the expression of repair genes. This modulation converts pro-inflammatory macrophages to reparative macrophages in the context of AP.

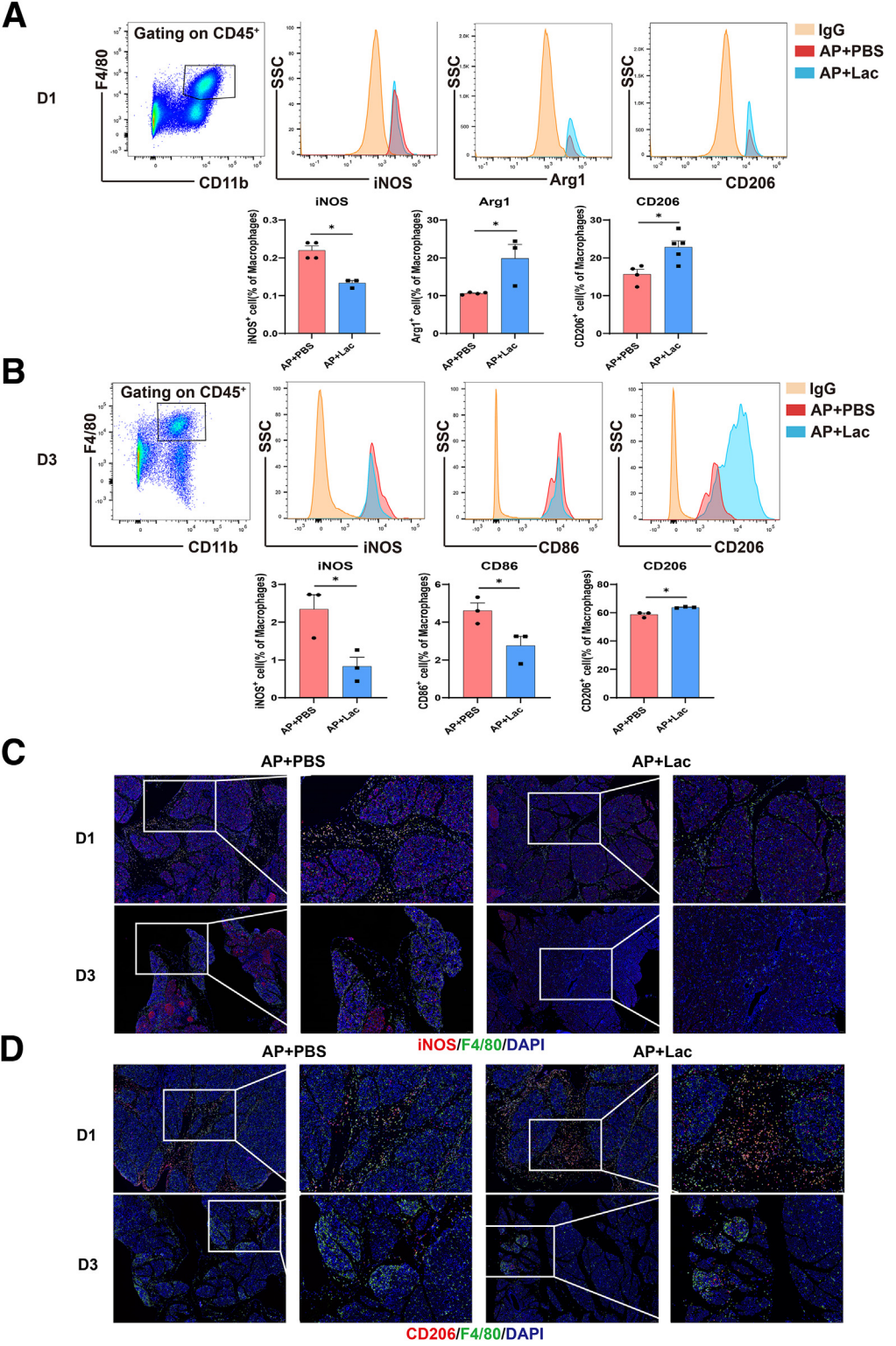
Together, lactate promotes histone H3 lactylation through MCT1 and inhibiting the JAK2-STAT1 signaling pathway via the GPR132 receptor. The combined effect facilitates the transition of macrophages from a pro-inflammatory to a reparative phenotype, improving the inflammatory immune microenvironment and ultimately promoting pancreatic repair following AP (Figure 13).

Notably, our experimental findings indicate that lactate promotes pancreatic repair following AP, contradicting previous reports of its pro-inflammatory role in chronic inflammation. In general, acute and chronic inflammation represent distinct inflammatory responses, characterized by different mechanisms and significant differences in disease progression, immune response, pathologic manifestations, and prognosis.⁵¹ These differences likely contribute to varying drug responses between acute and chronic inflammation. Specifically, the discrepancy regarding lactate's role in our experimental findings and previous studies on chronic inflammation may be attributed to 3 key factors: immune cell dynamics, spatiotemporal lactate exposure patterns, and inflammatory microenvironmental signatures.^{9,13,52} Furthermore, lactate not only plays distinct roles in acute and chronic inflammation but also exhibits varying effects within different chronic diseases. For instance, in rheumatoid arthritis, lactate disrupts T-cell homeostasis and enhances IL-17 production, exacerbating disease progression.^{53,54} In murine colitis models, however, intrarectal lactate administration reduces histopathologic damage and serum IL-6 levels.⁵⁵ These findings underscore that lactate's immunomodulatory function is context-dependent, exerting distinct regulatory effects across various chronic diseases.

Our study has certain limitations, as it primarily focused on the role and mechanisms of lactate in pancreatic repair following AP. Future studies should further investigate the dynamic changes in lactate between the inflammatory and repair phases of AP, as well as the coordination of functions between these phases, to gain a more comprehensive understanding of lactate's role in AP progression. Besides, among the lactylated proteins we identified, we have only

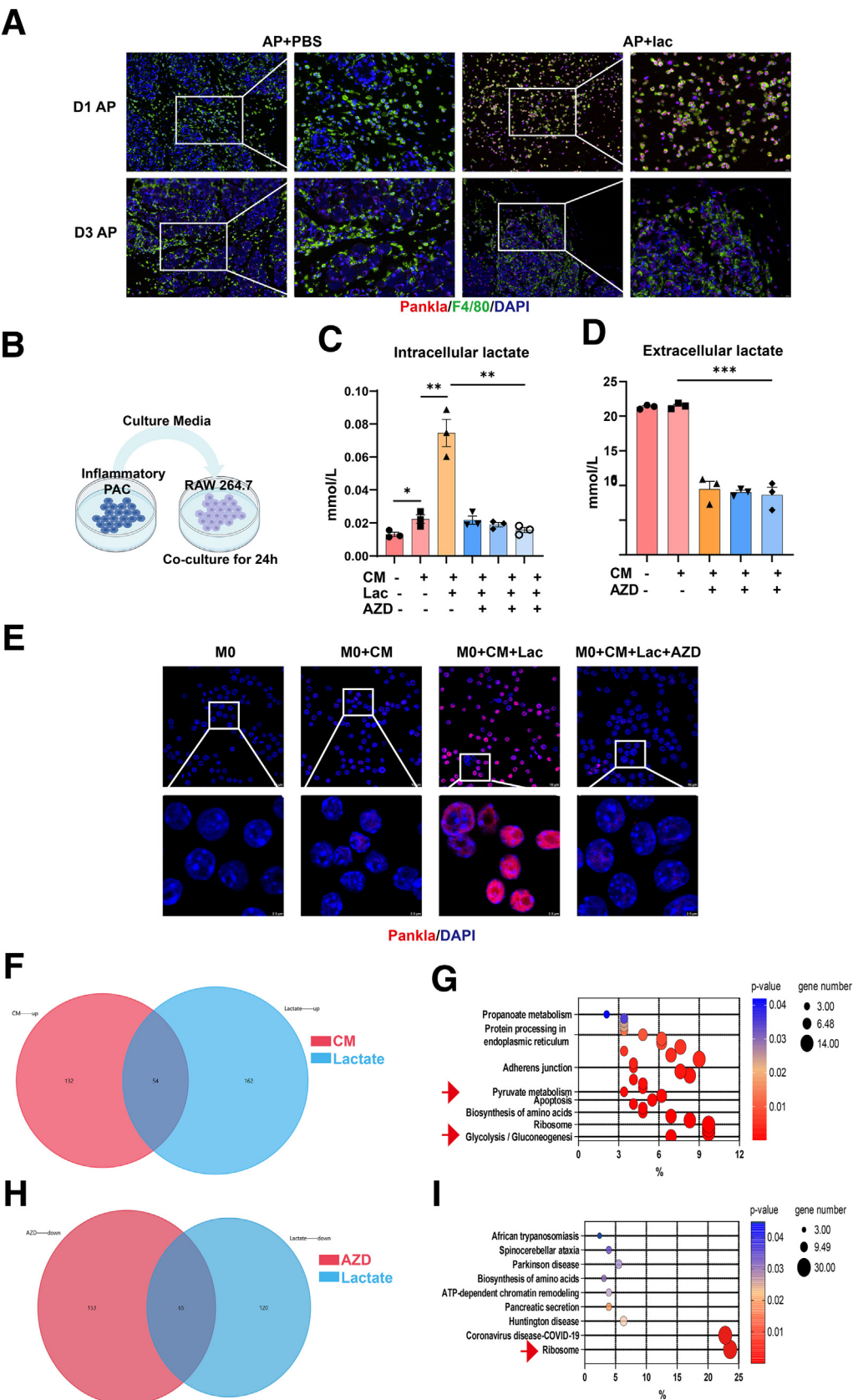
Figure 8. (See previous page). Lactate induces alterations in the phenotype of macrophages during the repair process following AP. (A) A schematic diagram illustrating the flow cytometry sorting process for macrophages in pancreatic tissue following the preparation of the RAP model. Subsequent RNA sequencing analysis was conducted. **(B)** Volcano plots illustrate the significantly differentially expressed genes ($P < .05$ and $|\text{Log}_2 \text{ Fold Change}| \geq 2$) between the AP + Lactate group and the AP + PBS group, $n = 3\text{--}4/\text{group}$. **(C–D)** Heat maps depicting differentially expressed genes associated with inflammation and repair in pancreatic macrophages on D1 (C) and D3 (D) during the recovery following AP in WT mice, $n = 3\text{--}4/\text{group}$. **(E–F)** GO enrichment analysis of significantly differentially expressed genes in macrophages from pancreatic tissue on D1 (E) and D3 (F), $n = 3\text{--}4/\text{group}$.

Figure 9. Lactate promotes the polarization of reparative macrophages during recovery following AP. (A–B) Flow cytometry analysis was performed to quantify the expression levels of macrophage markers: iNOS⁺, CD86⁺, Arg1⁺, CD206⁺ in pancreatic tissue on D1 (A) and D3 (B), n = 3–5/group. (C) Immunofluorescence analysis demonstrated the co-localization of iNOS (red) and F4/80 (green) in pancreatic tissue, DAPI (blue). The zoomed-in images represent high-magnification views of the outlined areas, with scale bars representing 50 μ m and 100 μ m, n = 5/group. (D) Immunofluorescence evaluation revealed the co-localization of CD206 (red) and F4/80 (green) in pancreatic tissue, DAPI (blue). The zoomed-in images represent high-magnification views of the outlined areas, with scale bars representing 50 μ m and 100 μ m, n = 5/group. Data are expressed as mean \pm SEM. Statistical significance is indicated as follows: **P* < .05.



verified and explored the functions of a select subset. Consequently, numerous proteins regulated by lactylation remain to be verified, and their functions require further exploration.

In summary, our findings demonstrate that lactate facilitates pancreatic repair following AP by promoting reparative macrophage polarization. This study advances our understanding of the role and mechanisms of lactate in



pancreatic repair following AP and offers valuable insights for improving AP treatment strategies.

Materials and Methods

Reagents

Cerulein (cat# HY-A0190), AZD3965 (cat# HY-12750), and GRP132 antagonist 1 (cat# HY-157189) were purchased from MedChemExpress. Lactate (cat# L6402-1G) was obtained from Sigma-Aldrich Chemical. The primary antibodies used in this study are listed in Table 1.

Animals

SPF male C57BL/6J mice (6–8 weeks old, 20–22 g) were purchased from Shanghai SLAC Laboratory Animal Co, Ltd. Heterozygous *Pfkfb3* mice were generously provided by Professor Honglin Wang of the Shanghai Institute of Immunology, Translational Medicine Center, Shanghai General Hospital, Key Laboratory of Cell Differentiation and Apoptosis, Ministry of Education, Shanghai Jiao Tong University School of Medicine. The heterozygous *Pfkfb3* mice used in this study were 6 to 8 weeks old, weighed 20 to 22 g, and were matched with WT littermates of the same sex, used consistently as controls. The *Pfkfb3* heterozygous mice were genotyped using previously established protocols.²⁷ All mice were housed under a 12-hour light/dark cycle at 22 °C with unrestricted access to standard food. Efforts were made to minimize pain and distress in the mice, and no adverse events were observed. All animal experiments were conducted following the principles of replacement, refinement, and reduction (3Rs) and in compliance with animal welfare regulations, adhering to ARRIVE guidelines and approved by the Animal Ethics Committee of Shanghai General Hospital (2023AW069).

RAP Model Construction and Intervention

Mice received intraperitoneal injections of cerulein (100 µg/kg) administered 8 times over 2 consecutive days at 1-hour intervals; the control group received an equivalent volume of saline. On the second day, lactate solution (504.3 µg/g) was administered intraperitoneally 10 hours after the initial cerulein injection, with the control group receiving an equal volume of PBS once daily. The lactate solution used was a 150 mM, pH 7.40 solution prepared in PBS.¹⁷ Mice

were sacrificed, and samples were collected on Day 0, 1, 3, 5, and 7 post-model preparation.

Lactate Level Measurement

The CheKine Micro Lactate Assay Kit (cat# KTB1100, Abbkine) was utilized to measure lactate levels in mouse serum, mouse monocytic cell line (RAW264.7), and culture supernatant. The lactate extraction reagent included in the kit was added to obtain the test sample. Both the sample and the lactate standard solution were transferred to a 96-well plate, followed by the addition of the reaction mixture. After incubating at 37 °C in the dark for 30 minutes, absorbance was measured at 450 nm in a microplate reader. The lactate concentration in the sample was then calculated by generating a standard curve of lactate concentration.

Hematoxylin and Eosin Staining and Scoring

Fresh pancreatic tissues were collected and fixed in 4% paraformaldehyde for 24 hours, after which they were sectioned into 4-µm slices for hematoxylin and eosin (H&E) staining according to standard procedures.^{29,56} Pancreatic tissues were scored on a scale of 0 to 5 by 2 experienced researchers in a blinded manner,⁵⁷ assessing parameters such as lobular integrity, acinar dedifferentiation, and inflammatory infiltration.

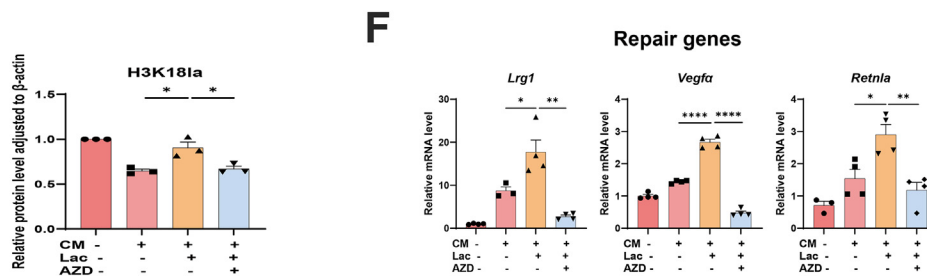
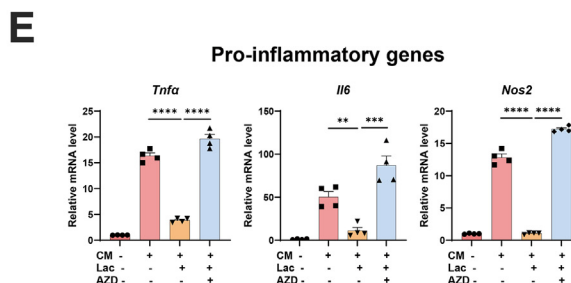
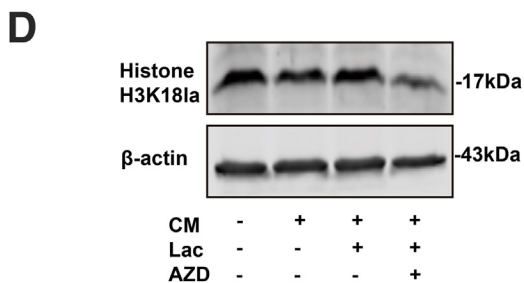
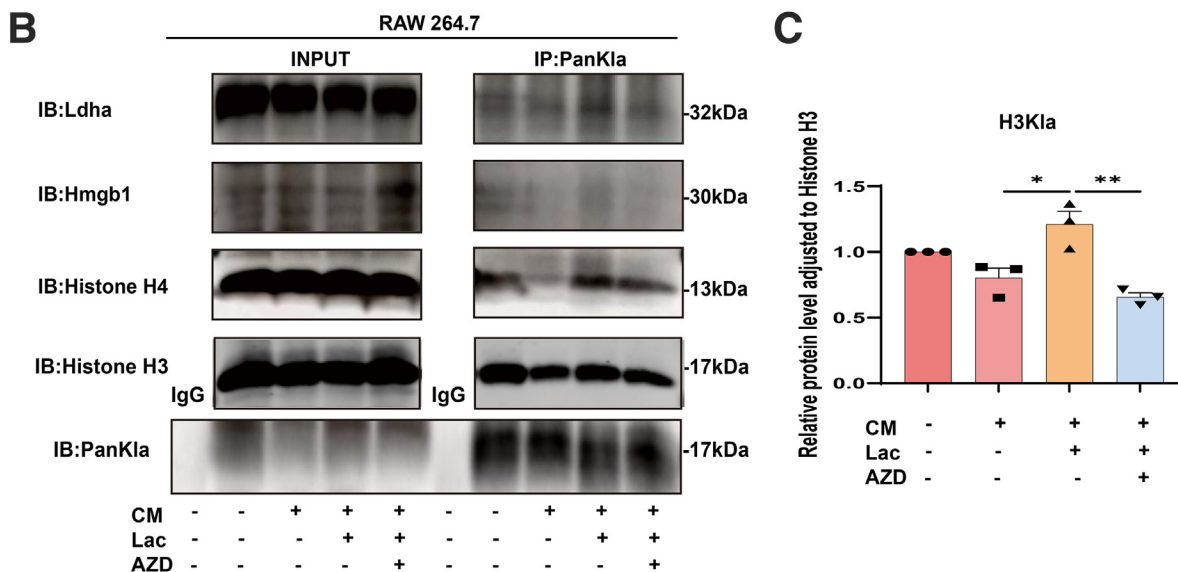
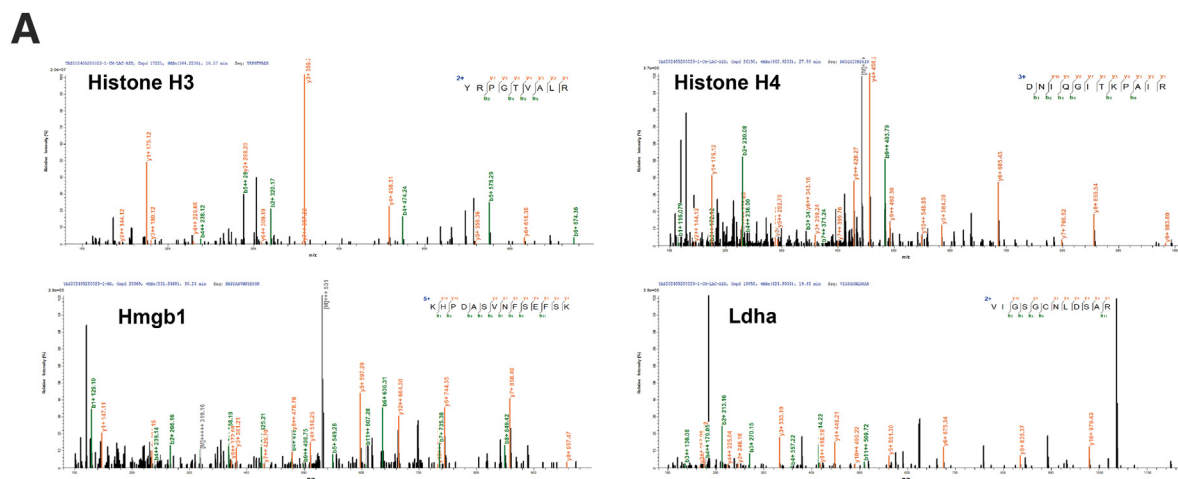
Serum Amylase and Lipase Assay

Serum was obtained by centrifuging at 1734 g for 15 minutes at 4 °C. Serum amylase and lipase levels were measured using a Roche/Hitachi modular analytics system (Roche Diagnostics).

Immunofluorescence

Paraffin-embedded pancreatic sections were dewaxed, rehydrated, and subjected to antigen retrieval by microwave in Citrate Antigen Retrieval Solution (Sangon Biotechnology).⁵⁶ Sections were then blocked with 10% goat serum for 1 hour. Subsequently, they were incubated overnight with primary antibodies. Following 3 washes with PBS, sections were incubated with secondary antibodies at 37 °C for 1 hour. Nuclei were counterstained with 4',6-diamidino-2-phenylindole (DAPI) for 10 minutes, and samples were mounted using fluorescent mounting medium

Figure 10. (See previous page). Lactate administration results in an increase in lactylation levels in macrophages. (A) Immunofluorescence staining was performed to examine the colocalization of lactylation (red) and F4/80 (green) in the pancreas on D1 and D3 during pancreatic repair after AP, DAPI (blue). The zoomed-in images represent high-magnification views of the outlined areas, with scale bars representing 10 µm and 20 µm, n = 5/group. (B) Schematic representation of the indirect in vitro co-culture system involving inflammatory primary acinar cells and the RAW 264.7 macrophage cell line. (C) Measurement of intracellular lactate levels in the macrophage cell line RAW 264.7, with conditions: Lactate (Lac) = 15 mM, AZD3965 (AZD) = 150 nM, 200 nM, and 250 nM from left to right, n = 3/group. (D) The levels of extracellular lactate were measured in the macrophage cell line RAW 264.7, with AZD drug concentrations indicated from left to right as 150 nM, 200 nM, and 250 nM, n = 3/group. (E) Immunofluorescence evaluation of lactylation (red) expression in macrophage cell line RAW 264.7, DAPI (blue). The zoomed-in images represent high-magnification views of the outlined areas, with scale bars representing 2.5 µm and 10 µm, AZD = 250 nM, n = 3/group. (F) Venn diagram illustrating the differentially expressed proteins among the various experimental comparisons. (G) KEGG pathway analysis of the significantly differentially expressed genes in the lactate treatment group. (H) A Venn diagram illustrates the differentially expressed proteins across comparisons. (I) KEGG pathway analysis was conducted on the significantly differentially expressed genes in the AZD group. Data are expressed as mean ± SEM. Statistical significance is indicated as follows: **P* < .05; ***P* < .01; and ****P* < .001.



(Yeasen Technology). Immunofluorescence staining results were visualized and analyzed with a Leica SP8 confocal microscope and LAS X software (Leica Application Suite X). Information on antibodies can be found in [Table 1](#).

Immunohistochemistry

After dewaxing and rehydrating, paraffin-embedded pancreatic sections underwent heat-induced antigen retrieval using Citrate Antigen Retrieval Solution (Sangon Biotechnology).⁵⁶ Sections were then blocked with 10% goat serum for 1 hour, followed by an overnight incubation with monoclonal antibodies against CD45 or F4/80. Visualization was achieved using an immunohistochemistry kit (Vector Laboratories). Information on antibodies can be found in [Table 1](#).

Western Blotting

Total proteins isolated from pancreatic tissue and RAW264.7 were extracted using a previously described method.^{56,58} Protein samples (40 μ g per lane) were subjected to 7.5%, 10%, or 12.5% sodium dodecyl sulfate-polyacrylamide gel electrophoresis (SDS-PAGE) (Epizyme Biotech) and subsequently electrotransferred to nitrocellulose membranes (Millipore). The membranes were incubated overnight at 4 °C with primary antibodies. Following this, samples were incubated with secondary antibodies for 1 hour at 37 °C. Target bands were visualized using the Odyssey CLx imaging system (LI-COR) or by ECL chemiluminescence and analyzed using Image J software. Information on antibodies can be found in [Table 1](#).

RT-qPCR

Total RNA was extracted from pancreatic tissue and RAW264.7 using Trizol reagent (cat# T9108, TakaRa) and subsequently reverse transcribed into complementary DNA (cDNA) using the Prime Script RT Reagent Kit (cat# RR037A, TakaRa). RT-qPCR was performed using SYBR Premix Ex Taq (cat# DRR420A, TakaRa) in a QuantStudio 7 Flex Real-Time PCR System (Applied Biosystems). Ribosomal protein lateral handle subunit P0 (*Rplp0*) served as the internal control. Relative mRNA expression was calculated using the comparative CT method ($2^{-\Delta\Delta CT}$). The mean values of the control group were set to 1, and values from all other groups were normalized relative to the control group and expressed as fold changes. All primers were purchased from Sangon Biotechnology and are detailed in [Table 2](#).

Enzyme-linked Immunosorbent Assay

The levels of inflammatory factors in mouse serum were determined using enzyme-linked immunosorbent

assay (ELISA) kits. Following the instructions for Il-6 (cat# EK206/3-96, Lianke Biotech), Tnf- α (cat# EK282/4-96, Lianke Biotech), and Il-1 β (cat# EK201B/3-96, Lianke Biotech), samples were added to the wells of the ELISA plate. The plate was then washed, followed by the addition of biotinylated anti-mouse monoclonal antibodies specific to Il-6, Tnf- α , and Il-1 β . After another washing step, horseradish peroxidase-labeled streptavidin was added, along with the substrate solution and stop solution. The absorbance values were read using an ELISA reader, and the levels of inflammatory factors in the samples were calculated by drawing a concentration standard curve.

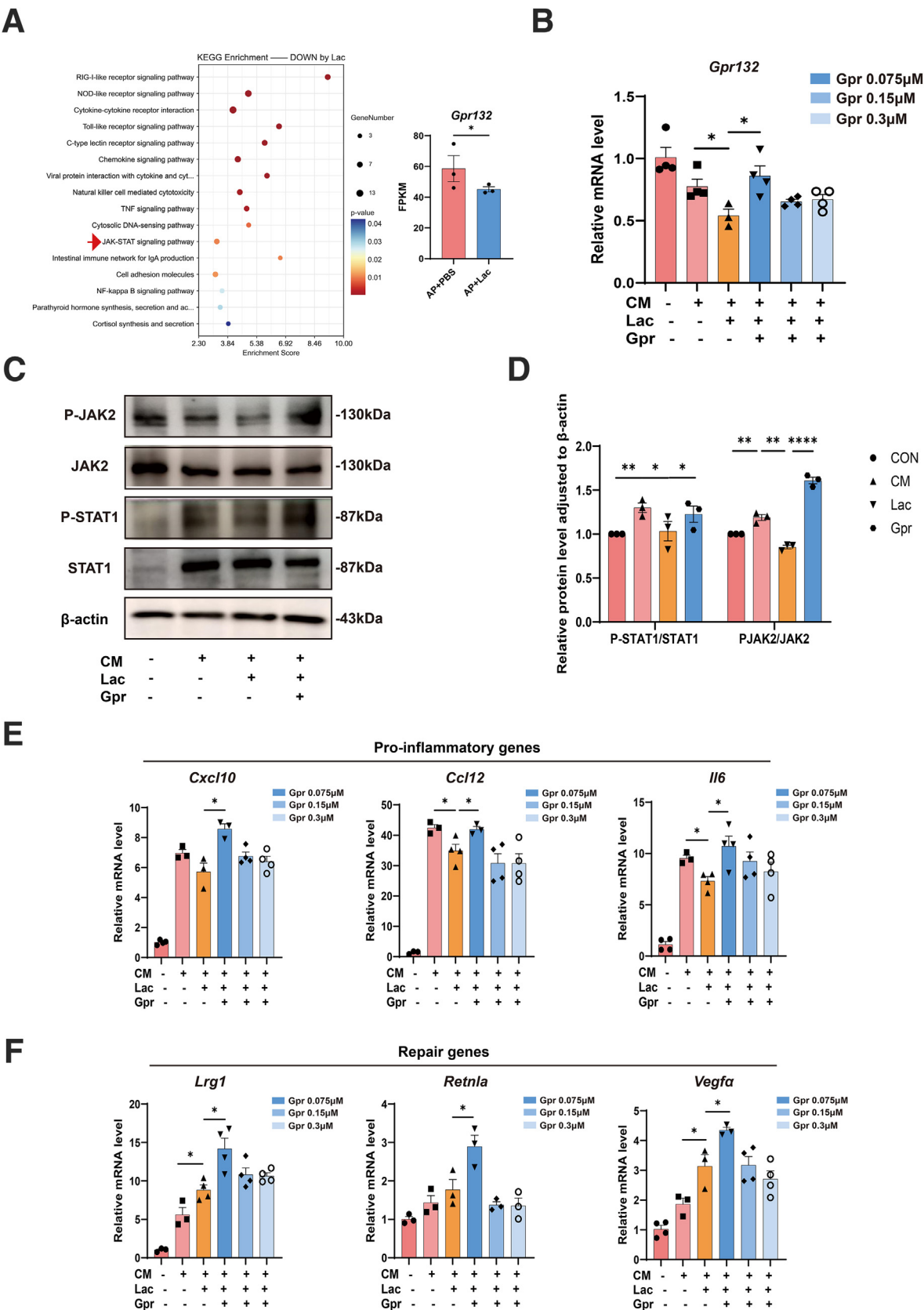
Primary Acinar Cell Isolation and Intervention

Mouse pancreatic tissue was digested using a modified collagenase IV isolation method, as previously described.^{56,59} Specifically, the pancreatic tissue was isolated, and 1 mL of collagenase IV (2 mg/mL, MP Bio-medicals) was injected at multiple points. The tissue was then incubated at 37 °C for 20 minutes and repeatedly agitated with a pipette tip with a cut end until the entire pancreatic tissue was completely dissociated. The digest was filtered through a 70- μ m cell sieve (Corning), centrifuged, washed, and resuspended in Dulbecco's Modified Eagle Medium (DMEM)/F-12 culture medium containing 10% fetal bovine serum (FBS) and antibiotics. After the acinar cells were isolated in vitro for 1 hour, they were stimulated with 400 mM cerulein for 3 hours to induce an in vitro model of AP.

Primary Acinar Cell 3D Culture and Intervention

The 3D culture of primary acinar cells was performed according to a previously described method.³¹ Specifically, after in vitro isolation, primary acini were resuspended in fresh 3D culture medium and embedded in Rat Tail Collagen I (cat# A1048301, Thermo Fisher Scientific), as described by Fleming Martinez et al.³¹ The 3D culture medium was refreshed every other day. The 3D medium consisted of DMEM/F-12 supplemented with 0.1 mg/mL trypsin inhibitor (cat# T9003, Sigma Aldrich), 1% FBS, 1 μ g/mL dexamethasone (cat# D4902, Sigma Aldrich), 50 ng/mL TGF- α (cat#HY-P77857, MedChemExpress), penicillin, and streptomycin. After the cells were plated and stabilized for 2 hours, lactate solutions with concentrations of 10 mM, 20 mM, and 30 mM (pH 7.4) were added. The process of acinar-to-ductal metaplasia was then observed, photographed, and recorded under a light microscope.

Figure 11. (See previous page). Lactate increases lactylation level via MCT1 to regulate macrophage polarization. (A) Mass spectrometry detection of lactylated histone H3, histone H4, Hmgb1, Ldha. (B) Immunoprecipitation was employed to evaluate the lactylation levels of histone H3, histone H4, Hmgb1, and Ldha in macrophages, AZD = 250 nM. (C–D) Immunoprecipitation (C) and WB (D) assessing the levels of histone H3 lactylation in macrophages, n = 3/group, AZD = 250 nM. (E) qPCR analysis of pro-inflammatory gene (*Tnf α* , *Il-6*, *Nos2*) expression levels in macrophages, n = 4/group, AZD = 250 nM. (F) qPCR analysis of repair gene (*Lrg1*, *Vegf α* , *Retnla*) expression levels in macrophages, n = 3–4/group, AZD = 250 nM. Data are expressed as mean \pm SEM. Statistical significance is indicated as follows: **P* < .05; ***P* < .01; ****P* < .001; and *****P* < .0001.



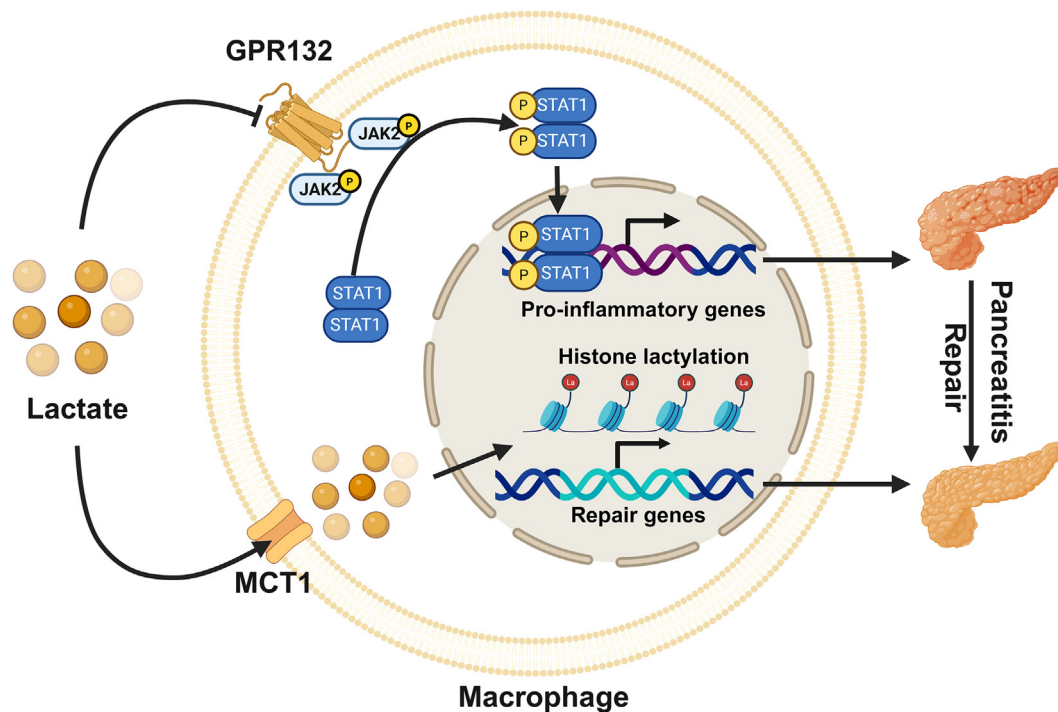


Figure 13. Mechanistic scheme.

Fluorescence-activated Cell Sorting

Mouse pancreatic tissue was obtained, cut into pieces, and washed with Hank's balanced solution containing 10% FBS. The tissue was then resuspended in Hank's balanced solution containing 2 mg/mL type IV collagenase and 10% FBS and incubated on a shaker at 37 °C for 15 minutes. The suspension was briefly vortexed at low speed for 20 seconds, centrifuged, and the supernatant was collected. Red blood cells were lysed using red blood cell lysis buffer (BD Pharmingen). The remaining cells were washed with Hank's balanced solution containing 2% FBS, followed by staining with anti-BV421-conjugated CD45, fluorescein isothiocyanate (FITC)-conjugated CD11b, and PE-Cyanine7-conjugated F4/80 antibodies for cell surface antigen labeling. Samples were incubated at 4 °C in the dark for 30 minutes, and CD45⁺CD11b⁺F4/80⁺ cells, indicative of macrophages, were sorted by flow cytometry. Data acquisition was performed on a BD Fortessa, and results were analyzed using FlowJo software (Treestar, version 10.6.2). Information on antibodies can be found in [Table 1](#).

Flow Cytometry

Mouse pancreas tissue was obtained, cut into pieces, and washed with Hank's balanced solution containing 10% FBS. The tissue was resuspended in Hank's balanced solution containing 2 mg/mL type IV collagenase and 10% FBS, then incubated on a shaker at 37 °C for 15 minutes. The suspension was briefly vortexed at low speed for 20 seconds, centrifuged, and the supernatant was collected. Red blood cells were lysed using a red blood cell lysis buffer. The remaining cells were washed with Hank's balanced solution containing 2% FBS, centrifuged, and resuspended. Surface antigen staining was performed using APC-Cyanine7 conjugated anti-CD45, FITC-conjugated anti-CD11b, PE-Cyanine7 conjugated anti-F4/80, and BV605 conjugated anti-CD86 antibodies, followed by incubation at 4 °C in the dark for 30 minutes. After washing, a fixative was added, and the samples were fixed at 4 °C in the dark for 15 minutes. The cells were then resuspended in permeabilization solution and incubated at 4 °C in the dark for 30 minutes with intracellular protein fluorescent antibodies, including PE-conjugated anti-iNOS, APC-conjugated anti-ARG1, and

Figure 12. (See previous page). Lactate inhibits the JAK2-STAT1 signaling pathway in macrophages through the GPR132 receptor, facilitating a switch in macrophage phenotype. (A) KEGG pathway analysis was conducted on significantly differentially expressed genes in pancreatic macrophages during recovery following AP in WT mice, alongside the mRNA expression levels of *Gpr132*, $n = 3/\text{group}$. (B) qPCR analysis of *Gpr132* mRNA expression in macrophages under lactate and GPR132 antagonist (0.075 μM , 0.15 μM , or 0.3 μM) treatment, Lactate (Lac) = 15 mM, $n = 3\text{--}4/\text{group}$. (C–D) WB analysis was performed to assess the expression levels of β -actin, STAT1, P-STAT1, JAK2, P-JAK2 (C), with the relative quantification (D), $n = 3/\text{group}$, Gpr = 0.075 μM . (E) qPCR detection of pro-inflammatory genes (*Cxcl10*, *Ccl12*, *Il6*) expression levels in macrophages following intervention with a GPR132 inhibitor, $n = 3\text{--}4/\text{group}$. (F) qPCR analysis of repair genes (*Lrg1*, *Retnla*, *Vegfa*) expression levels in macrophages post-intervention with a GPR132 inhibitor, $n = 3\text{--}4/\text{group}$. Data are expressed as mean \pm SEM. Statistical significance is indicated as follows: * $P < .05$; ** $P < .01$; *** $P < .001$; and **** $P < .0001$.

Table 1. Primary Antibodies Used in This Study

Type of experiment	Primary antibody	Obtained from	Cat. no	Dilution
IF	Amylase	SCB	sc-46657	1:100
IF	CK19	Abcam	ab52625	1:100
IF	SOX9	CST	82630	1:100
IF	Ki67	Abcam	ab16667	1:100
IF	F4/80	Proteintech	28463	1:4000
IF	iNOS	Proteintech	18985	1:800
IF	CD206	Abcam	ab64693	1:8000
IF	Pankla	PTM BIO	PTM-1401RM	1:100
IHC	CD45	CST	70257	1:100
IHC	F4/80	Proteintech	28463	1:1000
WB	AMYLASE	SCB	sc-46657	1:1000
WB	PFKFB3	Proteintech	13763-1-AP	1:1000
WB	Histone H3K18la	PTM BIO	PTM-1406RM	1:1000
WB	JAK2	Affinity	AF6022	1:500
WB	P-JAK2	Abcam	ab32101	1:1000
WB	STAT1	Affinity	AF6300	1:500
WB	P-STAT1	Affinity	AF3300	1:500
WB	β -ACTIN	Affinity	T0022	1:10000
WB	Histone H4	Abcam	ab10158	1:1000
WB	Histone H3	CST	4620S	1:1000
WB	LDHA	Proteintech	19987-1-AP	1:1000
WB	HMGB1	Proteintech	66525-1-Ig	1:1000
FC	BV421-conjugated anti-CD45	BioLegend	103134	1:100
FC	FITC-conjugated anti-CD11b	BioLegend	101206	1:100
FC	PE-Cyanine7-conjugated anti-F480	BioLegend	123114	1:50
FC	BV650-conjugated anti-CD206	BioLegend	141723	1:100
FC	PE-conjugated anti-iNOS	BioLegend	696806	1:100
FC	APC-Cyanine7-conjugated anti-CD45	BD Pharmingen	557659	1:100
FC	BV605-conjugated anti-CD86	BD Pharmingen	563055	1:100
FC	APC-conjugated anti-ARG1	Thermo Fisher Scientific	17-3697-82	1:100

CST, Cell Signaling Technology; FC, flow cytometry; FITC, fluorescein isothiocyanate; IF, immunofluorescence; IHC, immunohistochemistry; SCB, Santa Cruz Biotechnology; WB, Western blot.

BV650-conjugated anti-CD206. Following another wash, samples were analyzed by flow cytometry to confirm macrophage phenotypes based on the expression of iNOS, CD86, CD206, and ARG1. Data acquisition was performed on a BD Fortessa, and results were analyzed using FlowJo software (Treestar, version 10.6.2). Information on antibodies can be found in [Table 1](#).

Macrophage Culture and Intervention

The mouse monocytic cell line RAW264.7 was obtained from the Cell Bank of the Chinese Academy of Sciences. Cells were cultured in DMEM high-glucose medium supplemented with 10% FBS, penicillin, and streptomycin. The culture medium from acinar cells induced with AP in vitro was added and co-stimulated with lactate (15 mM) and AZD3965 (150 nM, 200 nM, or 250 nM) for 24 hours, or co-stimulated with lactate (15 mM) and GPR132 antagonist (0.075 μ M, 0.15 μ M, or 0.3 μ M) for either 6 or 24 hours.

Immunoprecipitation

Macrophages were digested and centrifuged, followed by the addition of cell lysis buffer. Proteins were lysed at 4 °C for 1 hour, after which 2 μ g of Pankla antibody or 2 μ g of IgG was added, and the samples were incubated at 4 °C overnight. The next day, Protein A+G Agarose (cat# P2055, Beyotime) was added and incubated at 4 °C for 6 hours. The samples were centrifuged, and the supernatant was discarded. After washing 3 times, protein loading buffer was added, and the samples were heated at 100 °C for 10 minutes. After centrifugation, the supernatant containing the target and binding proteins was collected for WB analysis. Information on antibodies can be found in [Table 1](#).

Statistical Analyses

Data are presented as mean \pm standard error of the mean (SEM). Intergroup comparisons were conducted using either Student's *t* test or analysis of variance (ANOVA). Statistical

Table 2. Primers Used in RT-qPCR

Genes	Forward	Reverse
<i>Rplp0</i>	CCACTTACTGAAAAGGTCAAGGC	CCTCCGACTCTTCCTTTGCT
<i>Il6</i>	GAGAGGAGACTTCACAGAGG	GTA CTCCAGAAGACCAGAGG
<i>Il1β</i>	ATGCCACCTTTTGACAGTGATG	TGATGTGCTGCTGCGAGATT
<i>Tnfα</i>	CCCACGTCGTAGCAAACCA	ACAAGGTACAACCCATCGGC
<i>Pfkfb3</i>	CAACTCCCCAACC GTGATTGT	TGAGGTAGCGAGTCAGCTTCT
<i>Ccnb1</i>	AGAGGTGGAAC TTGCTGAGCCT	GCACATCCAGATGTTTCCATCGG
<i>Krt19</i>	CCTCCCAGATTACAACCACT	AGGCGTGTCTGTCTCAAACCT
<i>Nos2</i>	GGTGAAGG GACTGAGCTGTT	ACGTTCTCCGTTCTCTTGCAG
<i>Lrg1</i>	CCTCAAGGAATGCCTGATACTG	GGAGAATTCCACCGACAGATG
<i>Retnla</i>	CAGCTGATGGTCCCAGTGAAT	CAGTGAGGGGATAGTTAGCTGG
<i>Vegfα</i>	GCAGACCAAAGAAAGACAGAAC	CAGTGAACGCTCCAGGATTTA
<i>Gpr132</i>	CCAATGCAGCAGGAACACC	CACGTTCTCTGCAGGACTT
<i>Cxcl10</i>	GTGAGAATGAGGGCCATAGG	GGCTAAACGCTTTCATTAAATTC
<i>Ccl12</i>	ATTCCACACTTCTATGCCTCCT	ATCCAGTATGGTCTCTGAAGATCA

RT-qPCR, reverse transcription quantitative polymerase chain reaction.

analyses were performed using GraphPad Prism 9.0 software, with a significance threshold set at $P < .05$. In vivo experiments were conducted with a minimum of 2 independent repetitions. The n values indicate the number of mice included in the analysis.

References

- Mederos MA, Reber HA, Girgis MD. Acute pancreatitis: a review. *JAMA* 2021;325:382–390.
- Zerem E. Treatment of severe acute pancreatitis and its complications. *World J Gastroenterol* 2014;20:13879–13892.
- Willemink M, Bollen T. Acute Pancreatitis. In: Hamm B, Ros PR, eds. *Abdominal Imaging*. Berlin Heidelberg: Springer, 2013:1337–1354.
- Kang R, Lotze MT, Zeh HJ, et al. Cell death and DAMPs in acute pancreatitis. *Mol Med* 2014;20:466–477.
- Zhu L, Xu Y, Lei J. Molecular mechanism and potential role of mitophagy in acute pancreatitis. *Mol Med* 2024;30:136.
- Hollemans RA, Hallensleben NDL, Mager DJ, et al, Dutch Pancreatitis Study Group. Pancreatic exocrine insufficiency following acute pancreatitis: systematic review and study level meta-analysis. *Pancreatology* 2018;18:253–262.
- Banks PA, Freeman ML. Practice Parameters Committee of the American College of Gastroenterology. Practice guidelines in acute pancreatitis. *Am J Gastroenterol* 2006;101:2379–2400.
- Glaubitz J, Asgarbeik S, Lange R, et al. Immune response mechanisms in acute and chronic pancreatitis: strategies for therapeutic intervention. *Front Immunol* 2023;14:1279539.
- Wu J, Zhang L, Shi J, et al. Macrophage phenotypic switch orchestrates the inflammation and repair/regeneration following acute pancreatitis injury. *EBioMedicine* 2020;58:102920.
- Ryu S, Lee EK. The pivotal role of macrophages in the pathogenesis of pancreatic diseases. *Int J Mol Sci* 2024;25:5765.
- Cruz AF, Rohban R, Esni F. Macrophages in the pancreas: villains by circumstances, not necessarily by actions. *Immun Inflamm Dis* 2020;8:807–824.
- Bruce JIE, Sánchez-Alvarez R, Sans MD, et al. Insulin protects acinar cells during pancreatitis by preserving glycolytic ATP supply to calcium pumps. *Nat Commun* 2021;12:4386.
- Luo Y, Li L, Chen X, et al. Effects of lactate in immunosuppression and inflammation: progress and prospects. *Int Rev Immunol* 2022;41:19–29.
- Noe JT, Rendon BE, Geller AE, et al. Lactate supports a metabolic-epigenetic link in macrophage polarization. *Sci Adv* 2021;7:eabi8602.
- Manosalva C, Quiroga J, Hidalgo AI, et al. Role of lactate in inflammatory processes: friend or foe. *Front Immunol* 2022;12:808799.
- Fang Y, Li Z, Yang L, et al. Emerging roles of lactate in acute and chronic inflammation. *Cell Commun Signal* 2024;22:276.
- Hoque R, Farooq A, Ghani A, et al. Lactate reduces liver and pancreatic injury in Toll-like receptor- and inflammasome-mediated inflammation via GPR81-mediated suppression of innate immunity. *Gastroenterology* 2014;146:1763–1774.
- Lee A, Ko C, Buitrago C, et al, NS-LR Study Group. Lactated ringers vs normal saline resuscitation for mild acute pancreatitis: a randomized trial. *Gastroenterology* 2021;160:955–957.e4.
- Wu BU, Hwang JQ, Gardner TH, et al. Lactated Ringer's solution reduces systemic inflammation compared with saline in patients with acute pancreatitis. *Clin Gastroenterol Hepatol* 2011;9:710–717.e1.

20. Buxbaum JL, Quezada M, Da B, et al. Early aggressive hydration hastens clinical improvement in mild acute pancreatitis. *Am J Gastroenterol* 2017;112:797–803.
21. Tenner S, Vege SS, Sheth SG, et al. American College of Gastroenterology Guidelines: management of acute pancreatitis. *Am J Gastroenterol* 2024;119:419–437.
22. Ngai D, Schilperoort M, Tabas I. Efferocytosis-induced lactate enables the proliferation of pro-resolving macrophages to mediate tissue repair. *Nat Metab* 2023; 5:2206–2219.
23. Zhang J, Muri J, Fitzgerald G, et al. Endothelial lactate controls muscle regeneration from ischemia by inducing M2-like macrophage polarization. *Cell Metab* 2020; 31:1136–1153.e7.
24. Zhang D, Tang Z, Huang H, et al. Metabolic regulation of gene expression by histone lactylation. *Nature* 2019; 574:575–580.
25. Bao J, Zhang X, Li B, et al. AXL and MERTK receptor tyrosine kinases inhibition protects against pancreatic necrosis via selectively limiting CXCL2-related neutrophil infiltration. *Biochim Biophys Acta Mol Basis Dis* 2022; 1868:166490.
26. Ge X, Cao Z, Gu Y, et al. PFKFB3 potentially contributes to paclitaxel resistance in breast cancer cells through TLR4 activation by stimulating lactate production. *Cell Mol Biol (Noisy-le-grand)* 2016;62:119–125.
27. Jiang H, Shi H, Sun M, et al. PFKFB3-driven macrophage glycolytic metabolism is a crucial component of innate antiviral defense. *J Immunol* 2016;197:2880–2890.
28. Murtaugh LC, Keefe MD. Regeneration and repair of the exocrine pancreas. *Annu Rev Physiol* 2015;77:229–249.
29. Dai J, Jiang M, Hu Y, et al. Dysregulated SREBP1c/miR-153 signaling induced by hypertriglyceridemia worsens acute pancreatitis and delays tissue repair. *JCI insight* 2021;6:e138584.
30. Paoli C, Carrer A. Organotypic culture of acinar cells for the study of pancreatic cancer initiation. *Cancers (Basel)* 2020;12:2606.
31. Fleming Martinez AK, Storz P. Mimicking and manipulating pancreatic acinar-to-ductal metaplasia in 3-dimensional cell culture. *J Vis Exp* 2019;144:59096.
32. Baldan J, Houbracken I, Rooman I, Bouwens L. Adult human pancreatic acinar cells dedifferentiate into an embryonic progenitor-like state in 3D suspension culture. *Sci Rep* 2019;9:4040.
33. Yang K, Fan M, Wang X, et al. Lactate promotes macrophage HMGB1 lactylation, acetylation, and exosomal release in polymicrobial sepsis. *Cell Death Differ* 2022;29:133–146.
34. Felmler MA, Jones RS, Rodriguez-Cruz V, et al. Monocarboxylate transporters (SLC16): function, regulation, and role in health and disease. *Pharmacol Rev* 2020; 72:466–485.
35. Végran F, Boidot R, Michiels C, et al. Lactate influx through the endothelial cell monocarboxylate transporter MCT1 supports an NF- κ B/IL-8 pathway that drives tumor angiogenesis. *Cancer Res* 2011;71:2550–2560.
36. Liu J, Zhao F, Qu Y. Lactylation: a novel post-translational modification with clinical implications in CNS diseases. *Biomolecules* 2024;14:1175.
37. Wang N, Wang W, Wang X, et al. Histone lactylation boosts reparative gene activation post-myocardial infarction. *Circ Res* 2022;131:893–908.
38. Zhang Y, Jiang H, Dong M, et al. Macrophage MCT4 inhibition activates reparative genes and protects from atherosclerosis by histone H3 lysine 18 lactylation. *Cell Rep* 2024;43:114180.
39. Shi W, Cassmann TJ, Bhagwate AV, et al. Lactic acid induces transcriptional repression of macrophage inflammatory response via histone acetylation. *Cell Rep* 2024;43:113746.
40. Xia T, Fu S, Yang R, et al. Advances in the study of macrophage polarization in inflammatory immune skin diseases. *J Inflamm (London)* 2023;20:33.
41. Banerjee S, Biehl A, Gadina M, et al. JAK-STAT signaling as a target for inflammatory and autoimmune diseases: current and future prospects. *Drugs* 2017;77:521–546.
42. Manohar M, Verma AK, Venkateshaiah SU, et al. Pathogenic mechanisms of pancreatitis. *World J Gastrointest Pharmacol Ther* 2017;8:10–25.
43. Chao KC, Chao KF, Chuang CC, Liu SH. Blockade of interleukin 6 accelerates acinar cell apoptosis and attenuates experimental acute pancreatitis in vivo. *Br J Surg* 2006;93:332–338.
44. Liu Y, Liu Z, Tang H, et al. The N(6)-methyladenosine (m(6)A)-forming enzyme METTL3 facilitates M1 macrophage polarization through the methylation of STAT1 mRNA. *Am J Physiol Cell Physiol* 2019; 317:C762–C775.
45. Chen P, Zuo H, Xiong H, et al. Gpr132 sensing of lactate mediates tumor-macrophage interplay to promote breast cancer metastasis. *Proc Natl Acad Sci U S A* 2017; 114:580–585.
46. Yu H, Lee H, Herrmann A, et al. Revisiting STAT3 signalling in cancer: new and unexpected biological functions. *Nat Rev Cancer* 2014;14:736–746.
47. Dai J, He Y, Jiang M, et al. Reg4 regulates pancreatic regeneration following pancreatitis via modulating the Notch signaling. *J Cell Physiol* 2021;236:7565–7577.
48. Li W, Zhou C, Yu L, et al. Tumor-derived lactate promotes resistance to bevacizumab treatment by facilitating autophagy enhancer protein RUBCNL expression through histone H3 lysine 18 lactylation (H3K18la) in colorectal cancer. *Autophagy* 2024; 20:114–130.
49. Pan R-Y, He L, Zhang J, et al. Positive feedback regulation of microglial glucose metabolism by histone H4 lysine 12 lactylation in Alzheimer's disease. *Cell Metabolism* 2022;34:634–648.e6.
50. Du S, Zhang X, Jia Y, et al. Hepatocyte HSPA12A inhibits macrophage chemotaxis and activation to attenuate liver ischemia/reperfusion injury via suppressing glycolysis-mediated HMGB1 lactylation and secretion of hepatocytes. *Theranostics* 2023;13:3856–3871.
51. Arulselvan P, Fard MT, Tan WS, et al. Role of antioxidants and natural products in inflammation. *Oxid Med Cell Longev* 2016;2016:5276130.
52. Rajendran P, Chen YF, Chen YF, et al. The multifaceted link between inflammation and human diseases. *J Cell Physiol* 2018;233:6458–6471.

53. Haas R, Smith J, Rocher-Ros V, et al. Lactate regulates metabolic and pro-inflammatory circuits in control of T cell migration and effector functions. *PLoS Biol* 2015;13:e1002202.
54. Subudhi I, Konieczny P, Prystupa A, et al. Metabolic coordination between skin epithelium and type 17 immunity sustains chronic skin inflammation. *Immunity* 2024;57:1665–1680.e7.
55. Iraporda C, Romanin DE, Bengoa AA, et al. Local treatment with lactate prevents intestinal inflammation in the TNBS-induced colitis model. *Front Immunol* 2016;7:651.
56. Li B, Wu J, Bao J, et al. Activation of $\alpha 7$ nACh receptor protects against acute pancreatitis through enhancing TFEB-regulated autophagy. *Biochim Biophys Acta Mol Basis Dis* 2020;1866:165971.
57. Folias AE, Penaranda C, Su AL, et al. Aberrant innate immune activation following tissue injury impairs pancreatic regeneration. *PLoS One* 2014;9:e102125.
58. Hu G, Shen J, Cheng L, et al. Reg4 protects against acinar cell necrosis in experimental pancreatitis. *Gut* 2011;60:820–828.
59. Wen L, Voronina S, Javed MA, et al. Inhibitors of ORAI1 prevent cytosolic calcium-associated injury of human pancreatic acinar cells and acute pancreatitis in 3 mouse models. *Gastroenterology* 2015;149:481–492.e7.

Received January 21, 2025. Accepted May 5, 2025.

Correspondence

Address correspondence to: Guoyong Hu, PhD, or Xingpeng Wang, PhD, Department of Gastroenterology, Shanghai General Hospital, 100 Haining Road, 200080 Shanghai, China. e-mail: richardwangxp@163.com; huguoyongsh@sina.com.

Acknowledgments

The authors thank professor Honglin Wang (Translational Medicine Center, Shanghai General Hospital) for providing *Pfkfb3*^{+/-} mice and professor Yiping Wang (Shanghai Key Laboratory of Pancreatic Disease, Shanghai General Hospital) for revising and providing suggestions for this manuscript. The

graphical abstract and schematic illustrations of mouse models were created using BioRender.

CRediT Authorship Contributions

Jing Jiang (Data curation: Lead; Formal analysis: Lead; Investigation: Lead; Methodology: Lead; Project administration: Lead; Software: Lead; Validation: Lead; Visualization: Lead; Writing – original draft: Lead; Writing – review & editing: Lead)

Ruiyan Wang (Data curation: Equal; Investigation: Equal; Methodology: Equal; Validation: Equal)

Pengli Song (Investigation: Equal; Methodology: Equal; Validation: Equal; Visualization: Equal)

Qi Peng (Investigation: Supporting; Methodology: Supporting; Validation: Supporting; Visualization: Supporting)

Xuerui Jin (Formal analysis: Supporting; Investigation: Supporting; Methodology: Supporting; Validation: Supporting; Visualization: Supporting)

Bin Li (Conceptualization: Supporting; Data curation: Supporting; Formal analysis: Supporting; Methodology: Supporting)

Jianbo Ni (Conceptualization: Supporting; Funding acquisition: Equal; Resources: Supporting; Supervision: Supporting)

Jie Shen (Conceptualization: Supporting; Formal analysis: Supporting; Methodology: Supporting; Supervision: Supporting)

Jingpiao Bao (Investigation: Supporting; Methodology: Supporting; Validation: Supporting; Visualization: Supporting)

Zengkai Wu (Conceptualization: Supporting; Formal analysis: Supporting; Methodology: Supporting; Resources: Supporting; Validation: Supporting)

Xiaolu Ge (Conceptualization: Supporting; Formal analysis: Supporting; Investigation: Supporting; Methodology: Supporting; Validation: Supporting)

Xingpeng Wang (Conceptualization: Equal; Funding acquisition: Lead; Project administration: Equal; Resources: Lead; Supervision: Equal)

Guoyong Hu, PhD, MD (Conceptualization: Lead; Funding acquisition: Lead; Project administration: Lead; Supervision: Lead; Writing – review & editing: Supporting)

Conflicts of interest

The authors disclose no conflicts.

Funding

This work was sponsored by the National Natural Science Foundation of China to Xingpeng Wang (8227032479) and the Shanghai Pujiang Programme (23PJD082) and the Science and Technology Innovation Action Plan of Shanghai Municipal Science and Technology Commission (23Y11902000) to Jianbo Ni.

Data Availability

The publicly available dataset supporting the findings of this study can be accessed in the National Center for Biotechnology Information Gene Expression Omnibus under accession code GSE191008 and GSE297476 for bulk RNA sequencing. All other data supporting the findings are available from the corresponding author upon reasonable request.